

Supplementary Information

Amino acid-derived bisphenolate palladium complexes as C-C coupling catalysts

*Eszter Fazekas, David T. Jenkins, Andrew A. Forbes, Brendan Gallagher, Georgina M. Rosair, Ruaraidh D. McIntosh**

Institute of Chemical Sciences, Heriot-Watt University, Edinburgh, EH14 4AS (UK)

Contents

- 1. ^1H and ^{13}C NMR spectra of pro-ligands L1-L6**
- 2. ESI High Resolution Mass Spectrometry data of pro-ligands L1-L6**
- 3. X-ray structures of pro-ligands L1-L6**
- 4. Data for the racemisation studies of pro-ligands L2, L3, L5 and L6**
- 5. ^1H and ^{13}C NMR spectra of Pd complexes C1-C7**
- 6. ESI High Resolution Mass Spectrometry data of Pd complexes C1-C7**
- 7. Typical ^1H NMR spectra of Suzuki-Miyaura and Mizoroki-Heck crude reaction mixtures**
- 8. Crystallographic data and refinement details for ligands L1-L6 and complexes C1-C6**
- 9. References**

1. ^1H and ^{13}C NMR spectra of pro-ligands L1-L6

L1

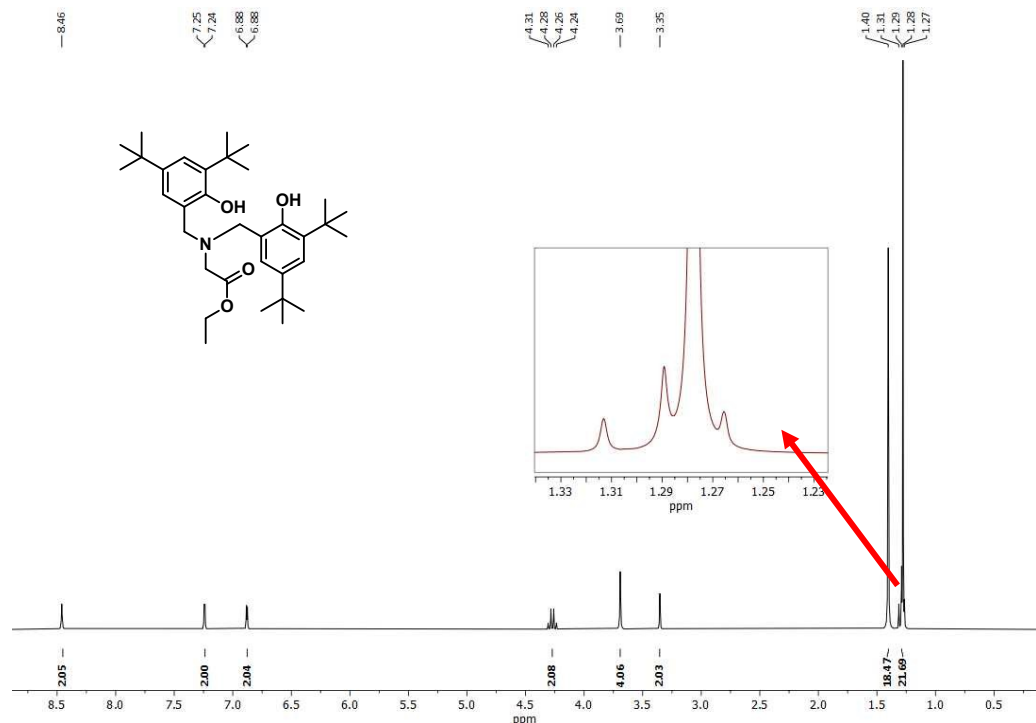


Figure S1. ^1H NMR spectrum of L1 (300 MHz, CDCl_3 at 298 K).

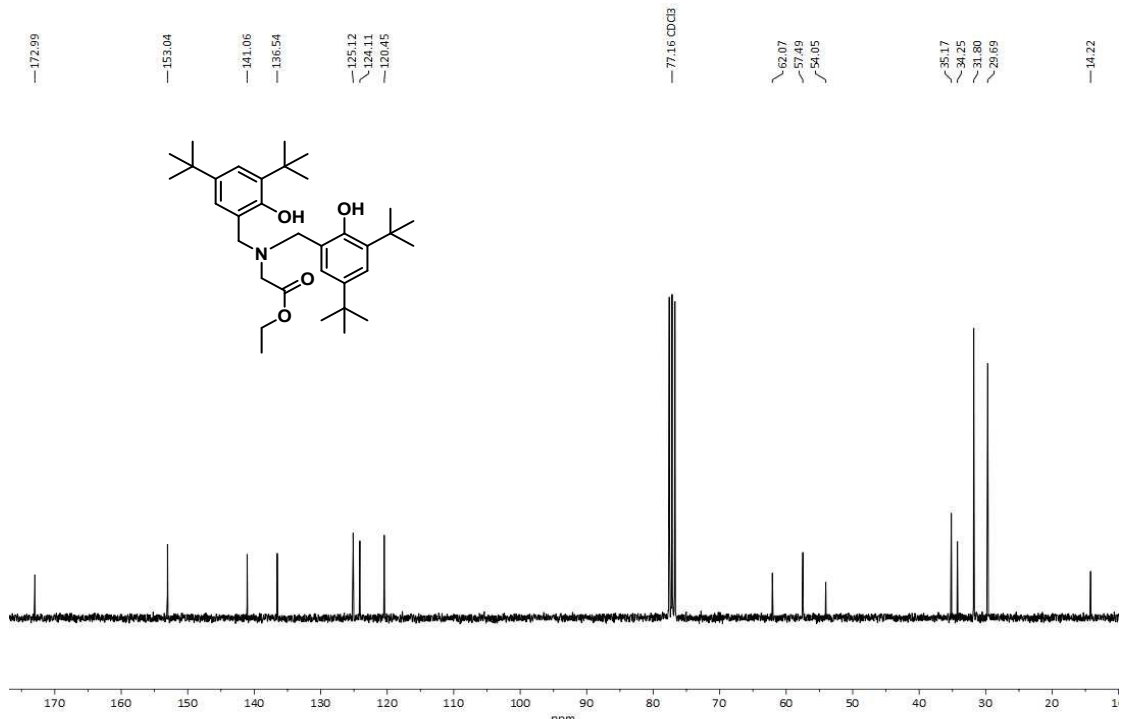


Figure S2. ^{13}C NMR spectrum of L1 (75 MHz, CDCl_3 at 298 K).

L2

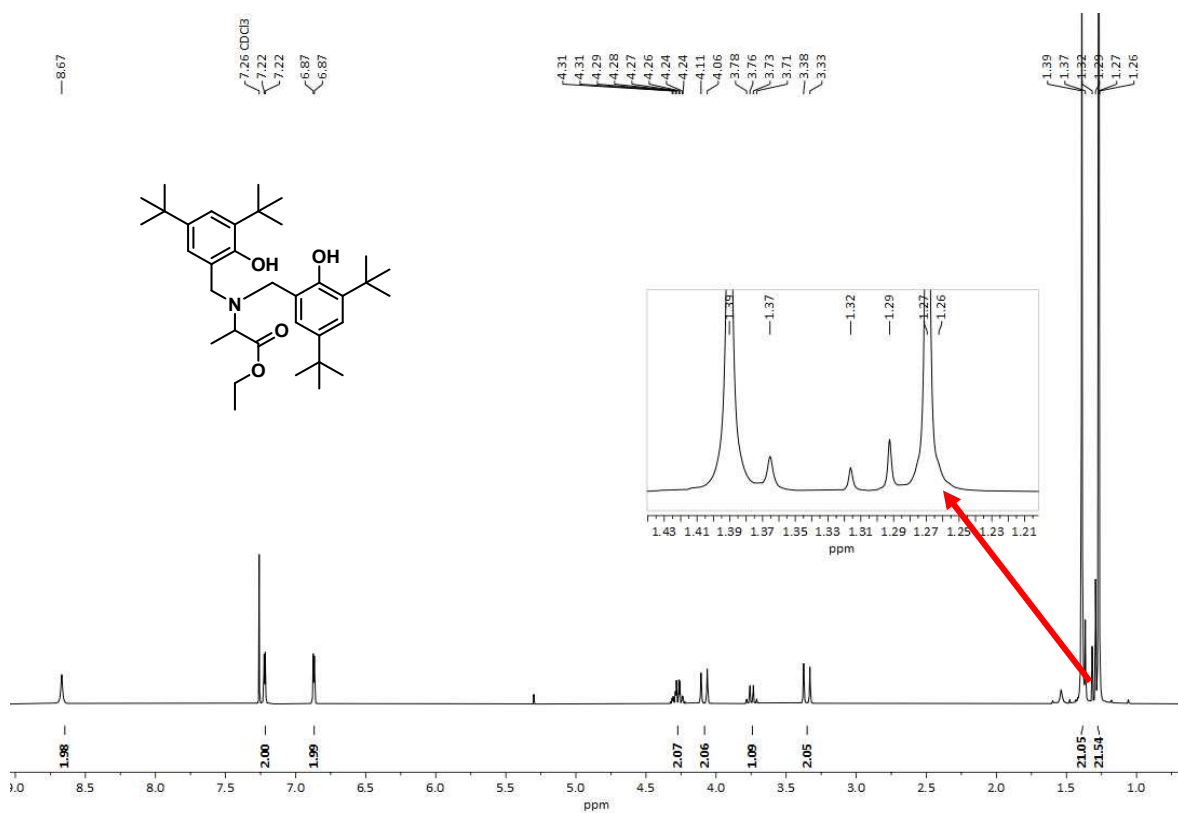


Figure S3. ¹H NMR spectrum of L2 (300 MHz, CDCl₃ at 298 K).

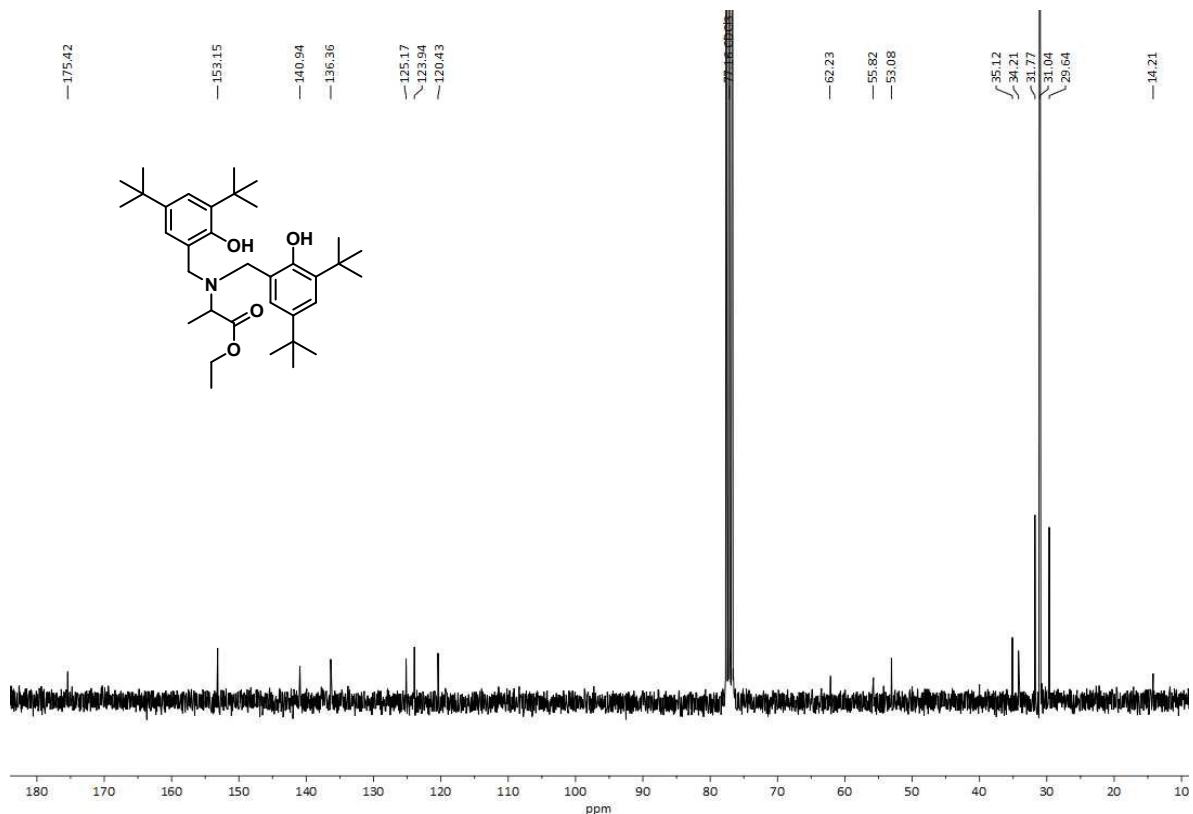


Figure S4. ¹³C NMR spectrum of L2 (75 MHz, CDCl₃ at 298 K).

L3

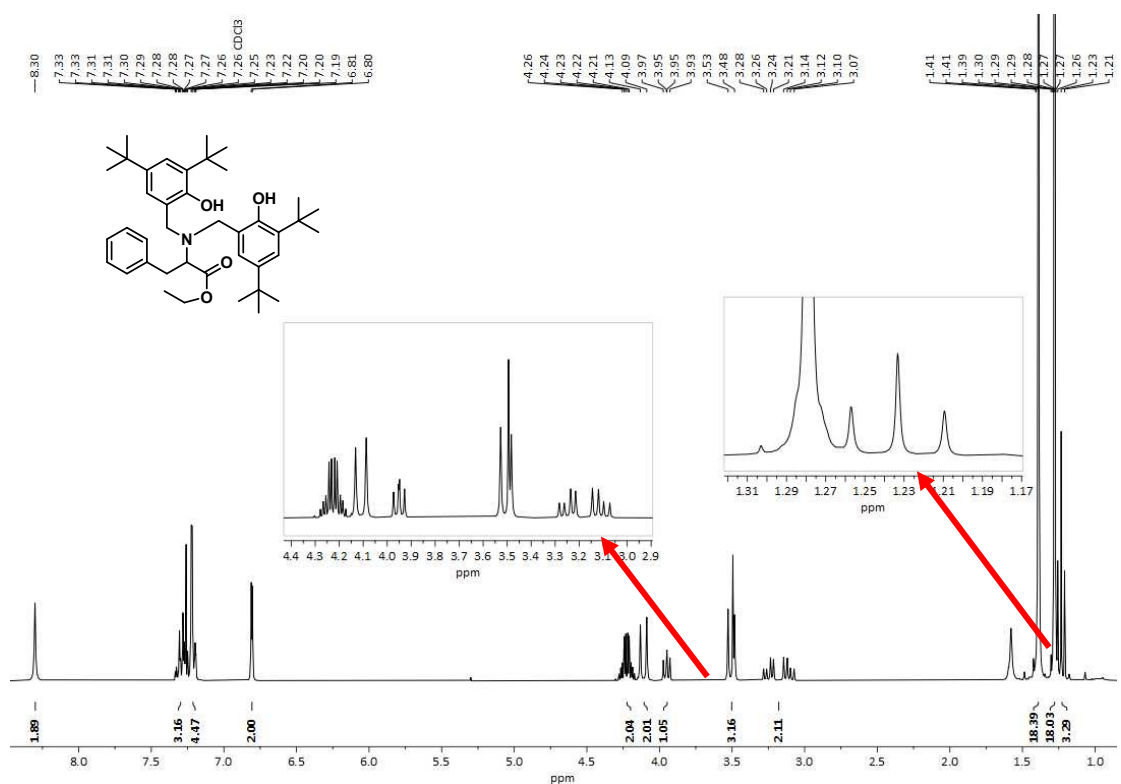


Figure S5. ¹H NMR spectrum of L3 (300 MHz, CDCl₃ at 298 K).

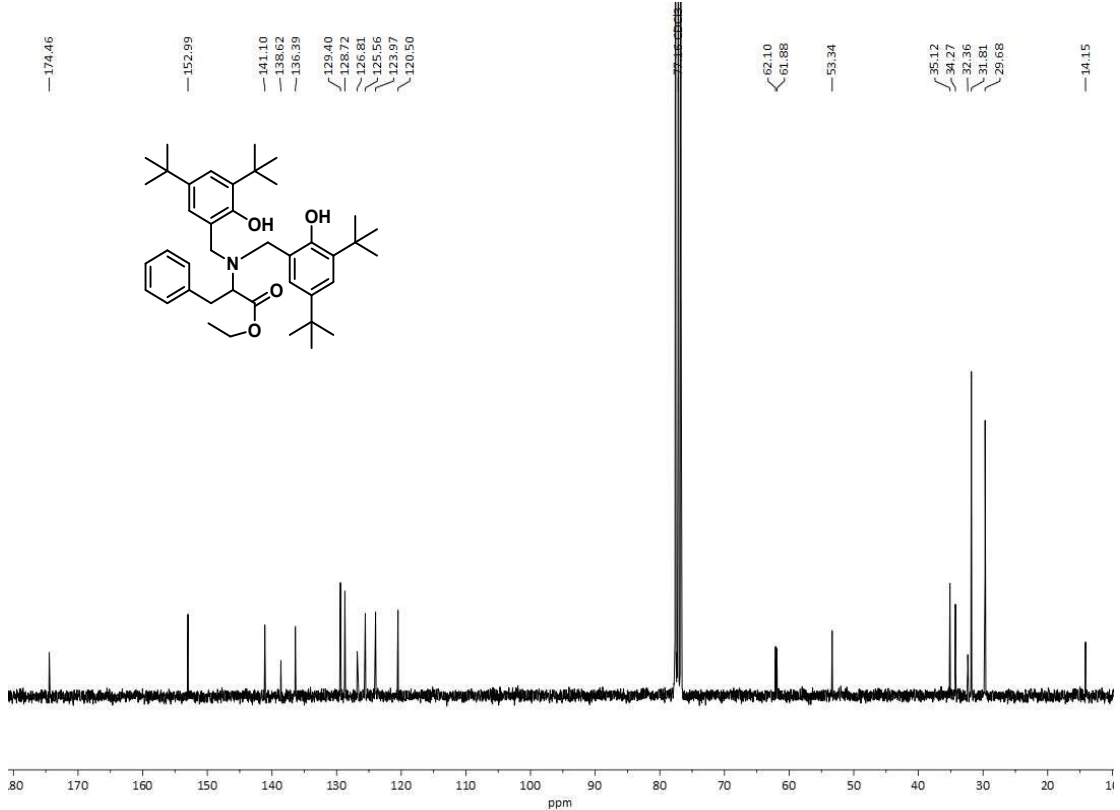


Figure S6. ¹³C NMR spectrum of L3 (75 MHz, CDCl₃ at 298 K).

L4

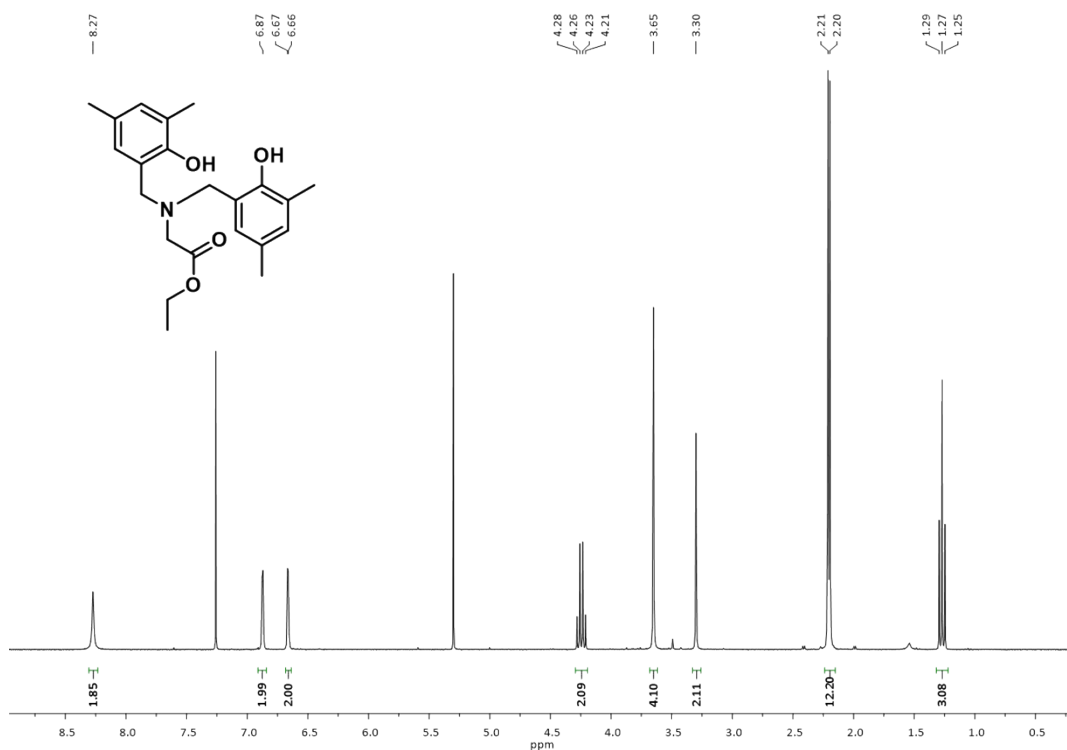


Figure S7. ¹H NMR spectrum of L4 (300 MHz, CDCl₃ at 298 K).

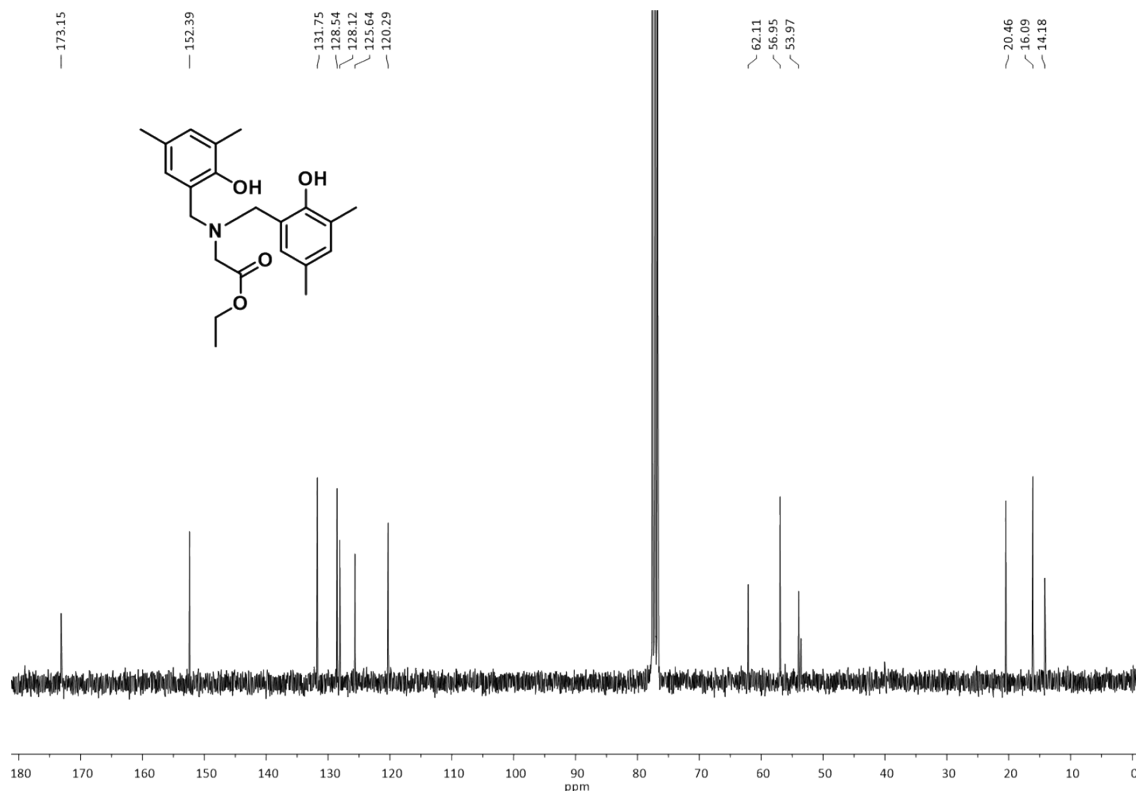


Figure S8. ¹³C NMR spectrum of L4 (75 MHz, CDCl₃ at 298 K).

L5

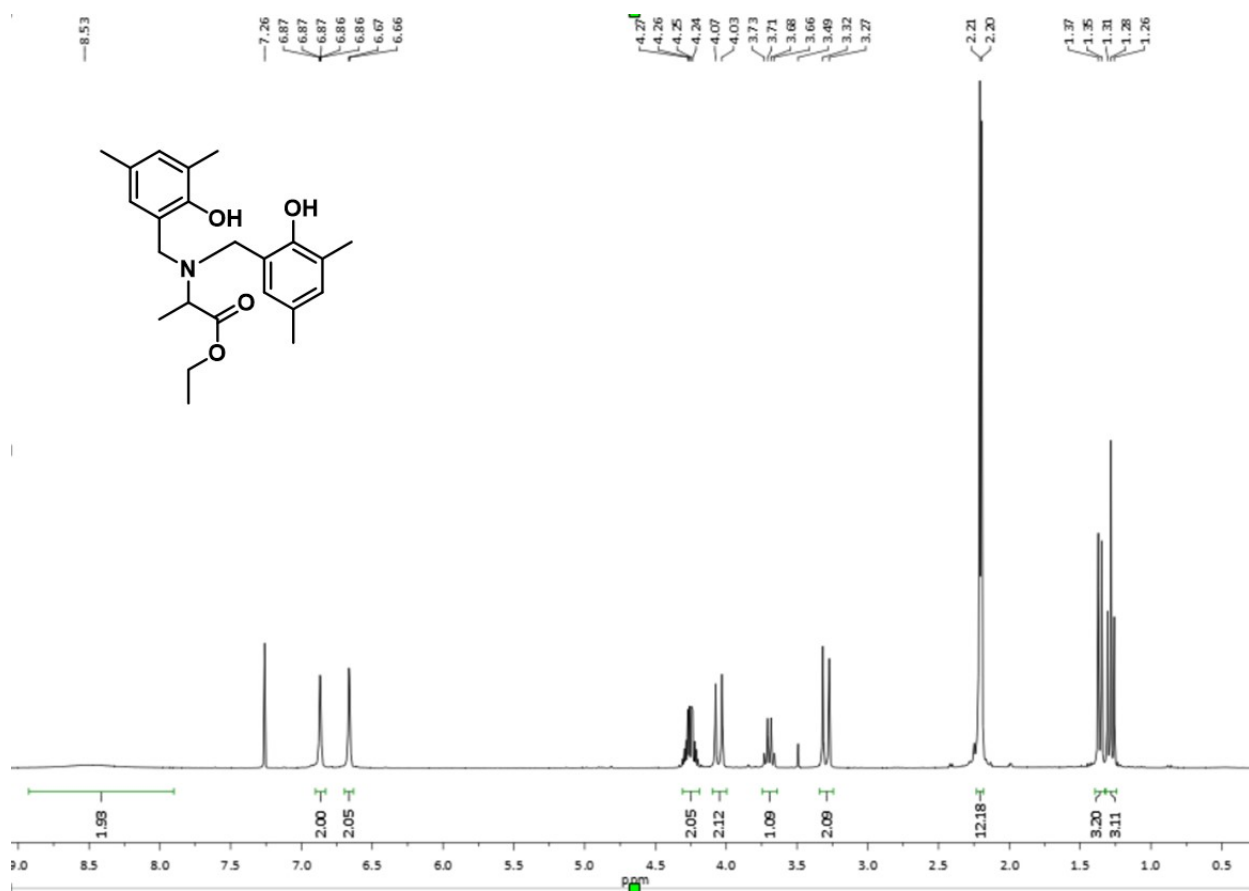


Figure S9. ^1H NMR spectrum of L5 (300 MHz, CDCl_3 at 298 K).

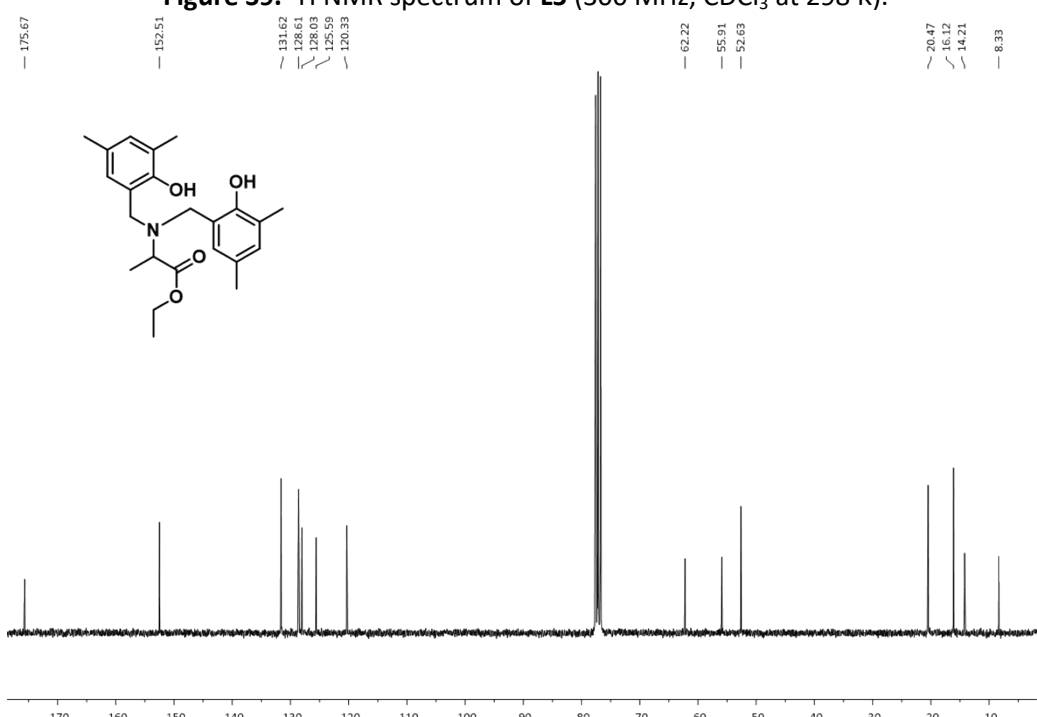


Figure S10. ^{13}C NMR spectrum of L5 (75 MHz, CDCl_3 at 298 K).

L6

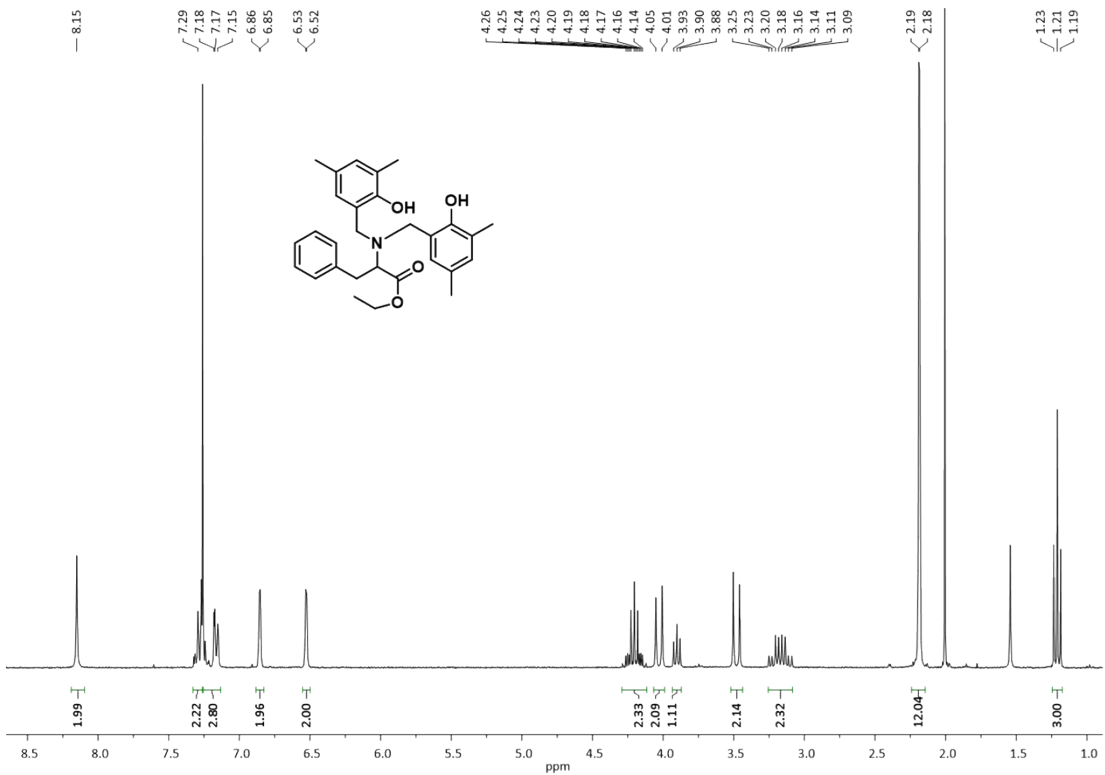


Figure S11. ¹H NMR spectrum of L6 (300 MHz, CDCl₃ at 298 K).

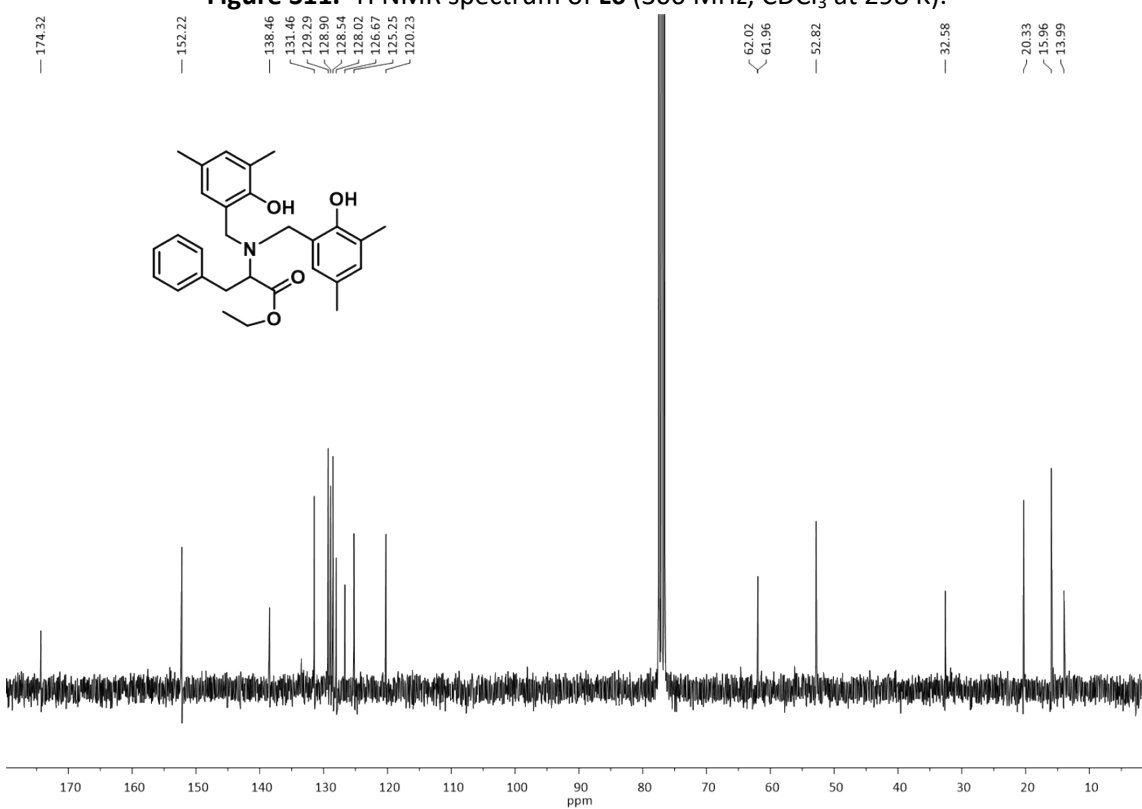


Figure S12. ¹³C NMR spectrum of L6 (75 MHz, CDCl₃ at 298 K).

2. ESI High Resolution Mass Spectrometry data of pro-ligands L1-L6

L1

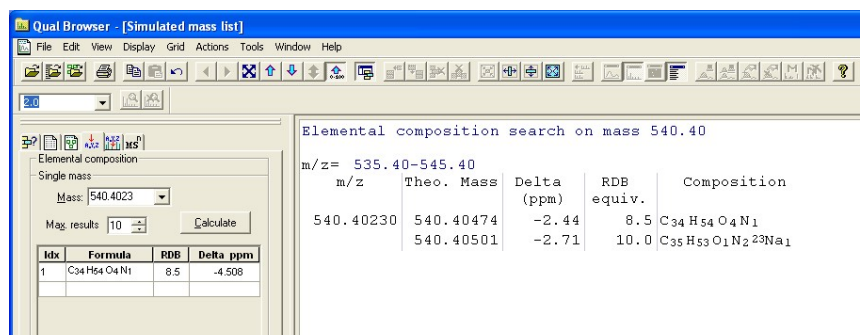


Figure S13. HRMS data of L1.

L2

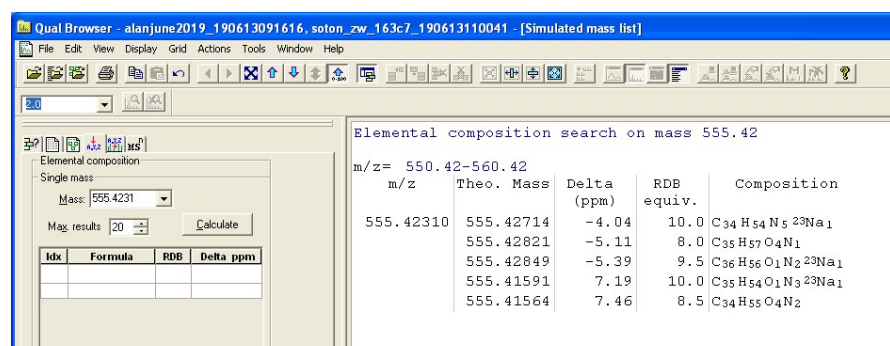


Figure S14. HRMS data of L2.

L3

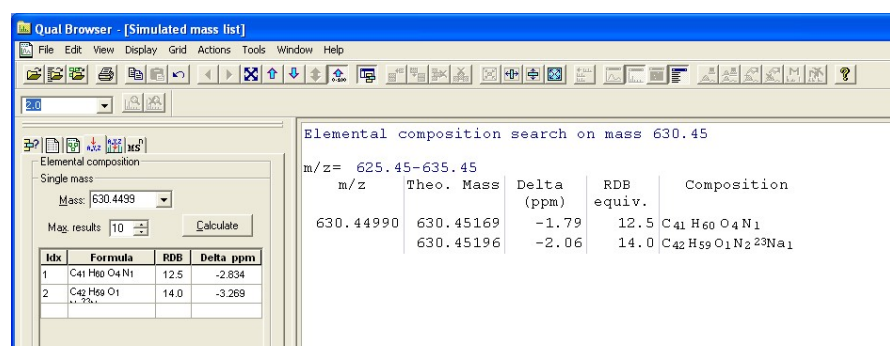


Figure S15. HRMS data of L3.

L4

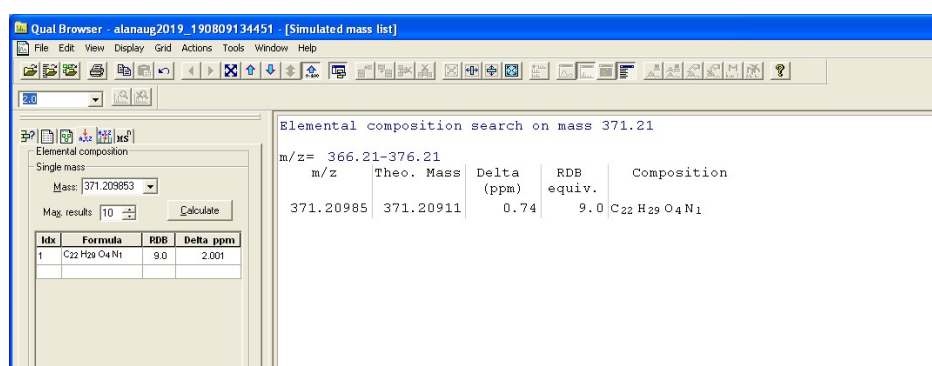


Figure S16. HRMS data of L4

L5

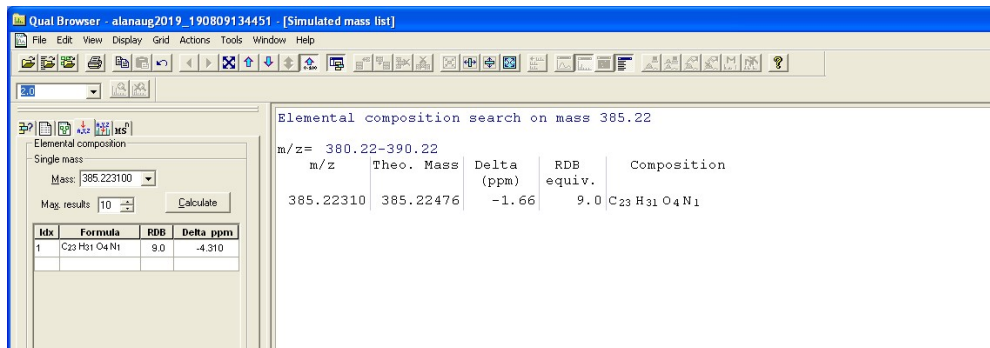


Figure S17. HRMS data of L5.

L6

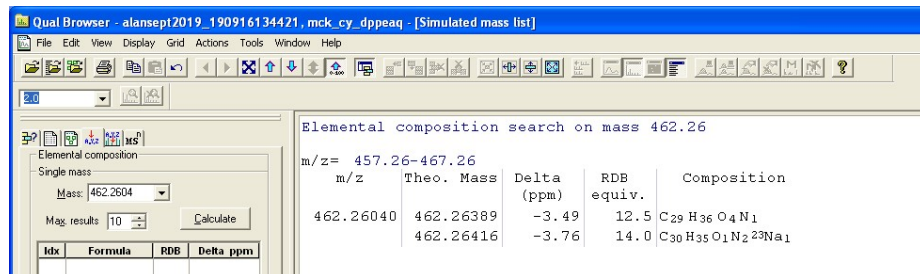


Figure S18. HRMS data of L6.

3. X-ray structures of pro-ligands L1-L6

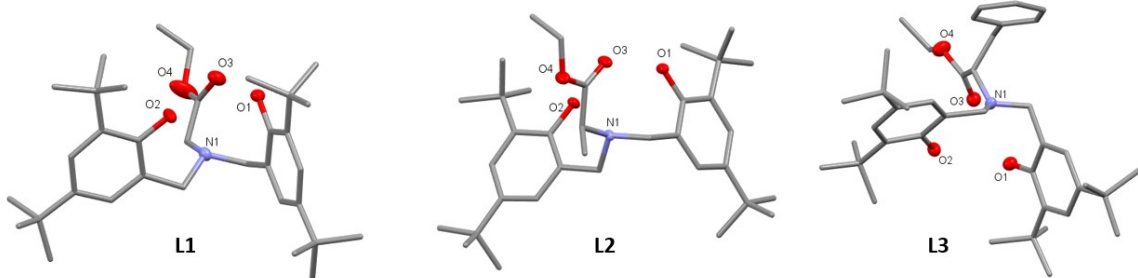


Figure S19. X-ray structures of L1, L2 and L3 (from left to right).

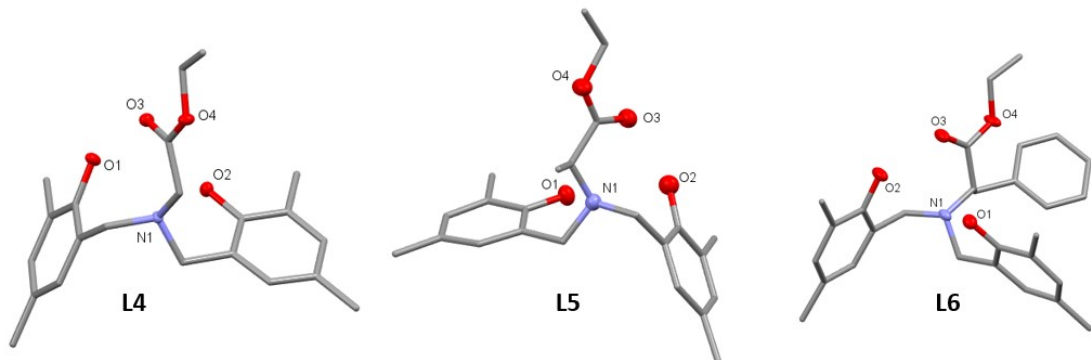


Figure S20. X-ray structures of L4, L5 and L6 (from left to right).

4. Data for the racemisation studies of chiral pro-ligands

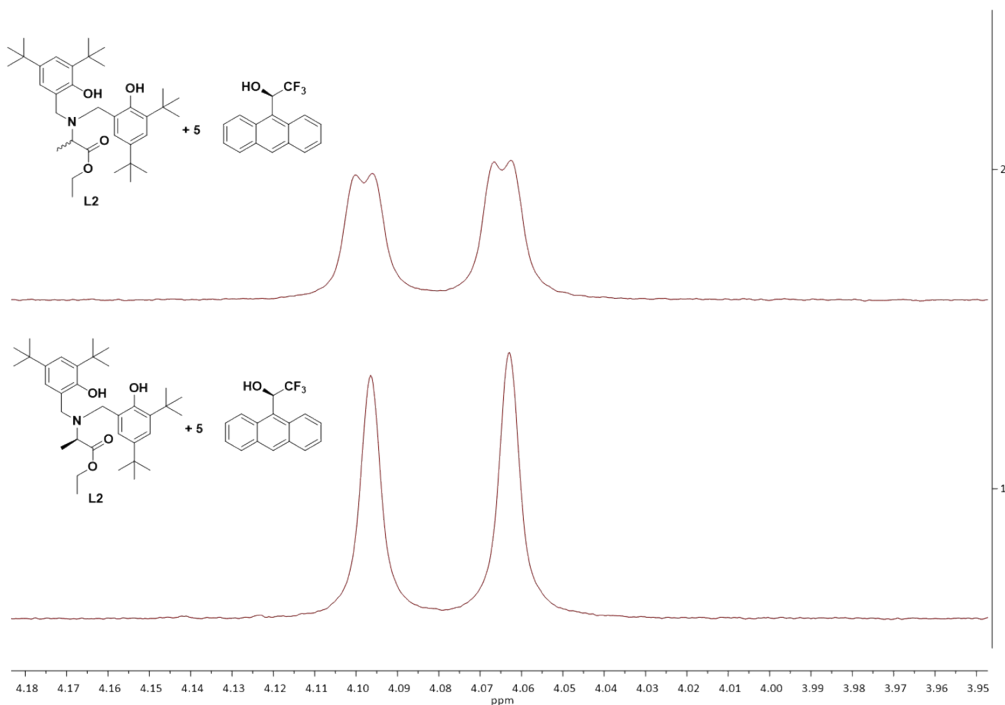


Figure S21. Comparison of the methylene resonances (4.08 ppm) in the ¹H NMR spectra of racemic (top) and enantiopure (bottom) pro-ligand L2 in the presence of 5 equivalents of (R)-(-)-1-(9-anthryl)-2,2,2-trifluoroethanol shift reagent (300 MHz, CDCl₃ at 298 K).

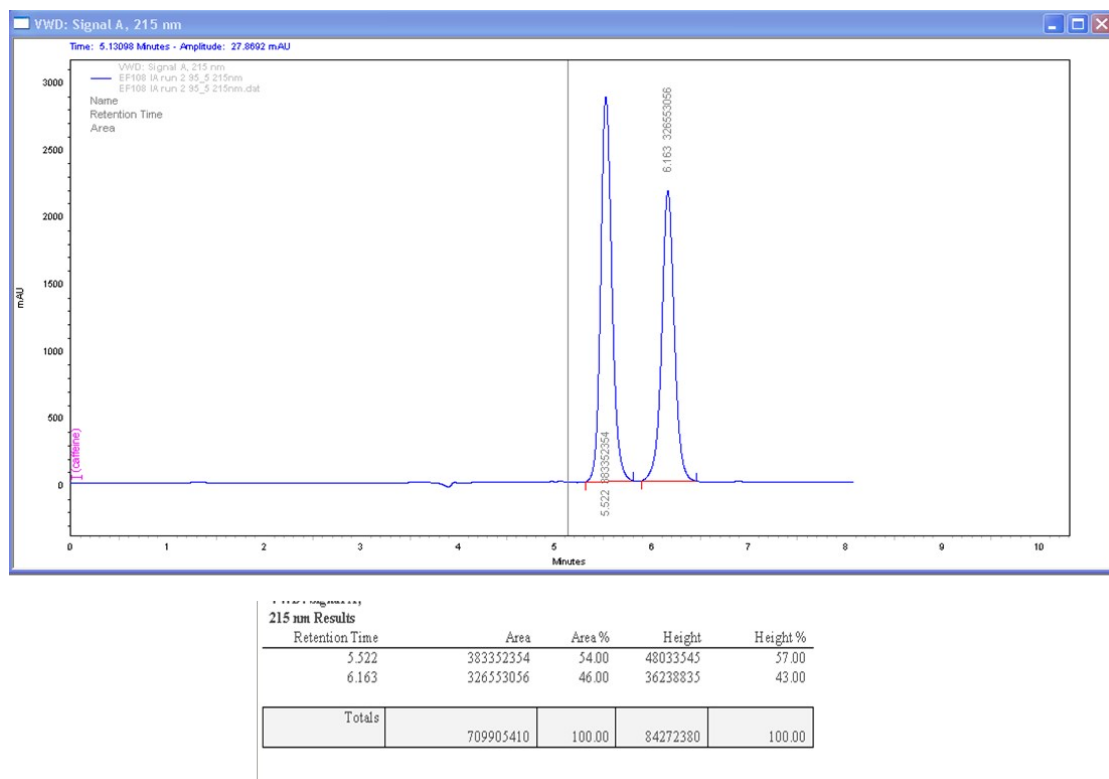


Figure S22. HPLC chromatogram of racemic pro-ligand L5 on CHIRALPAK IA column, hexane:2-propanol 95:5, flow rate: 1.0 mL min⁻¹, detection UV 215 nm, 298 K) t_R of isomers: 5.52 min and 6.16 min.

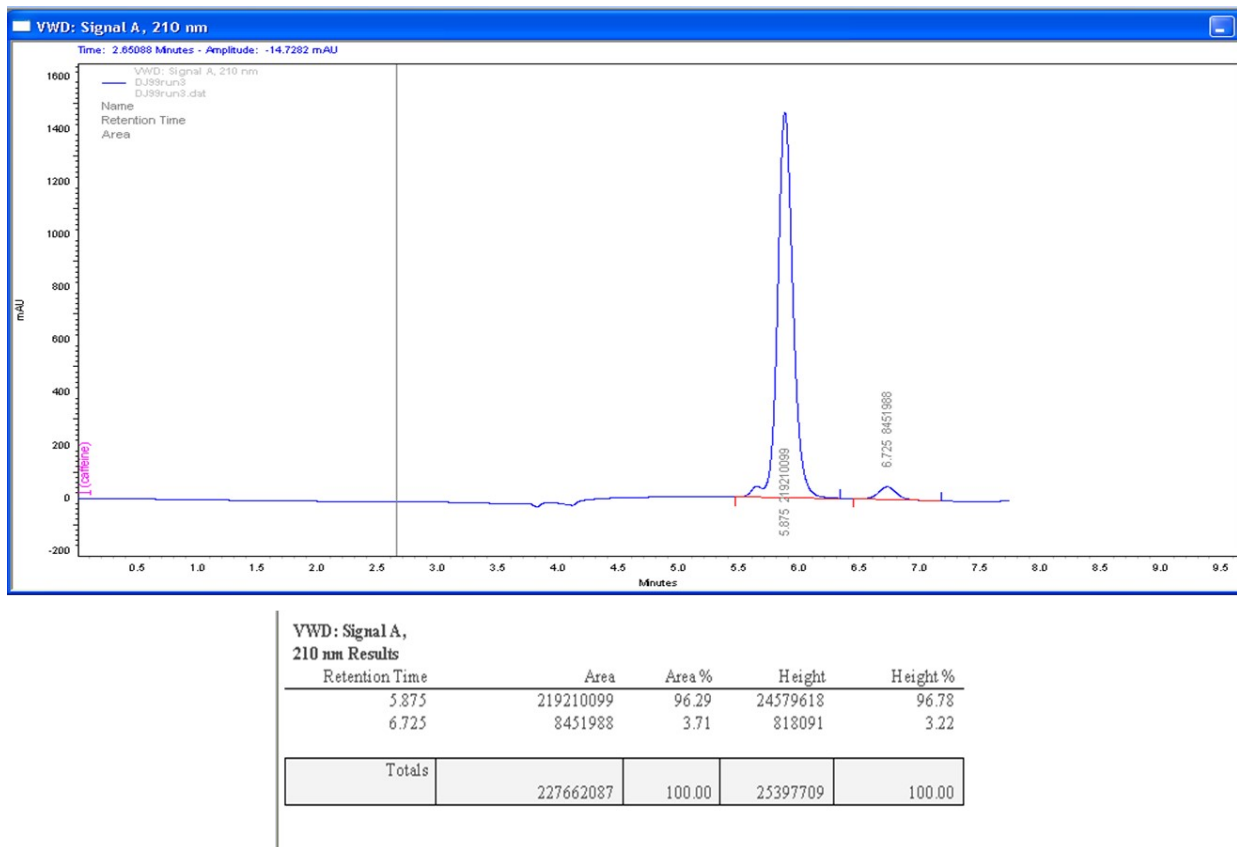


Figure S23. HPLC chromatogram of (L)-**L5** on CHIRALPAK IA column, hexane:2-propanol 95:5, flow rate: 1.0 mL min⁻¹, detection UV 215 nm, 298 K) t_R of major isomer: 5.87 min, t_R of minor isomer: 6.72 min.

5. ^1H and ^{13}C NMR spectra of Pd complexes C1-C7

C1

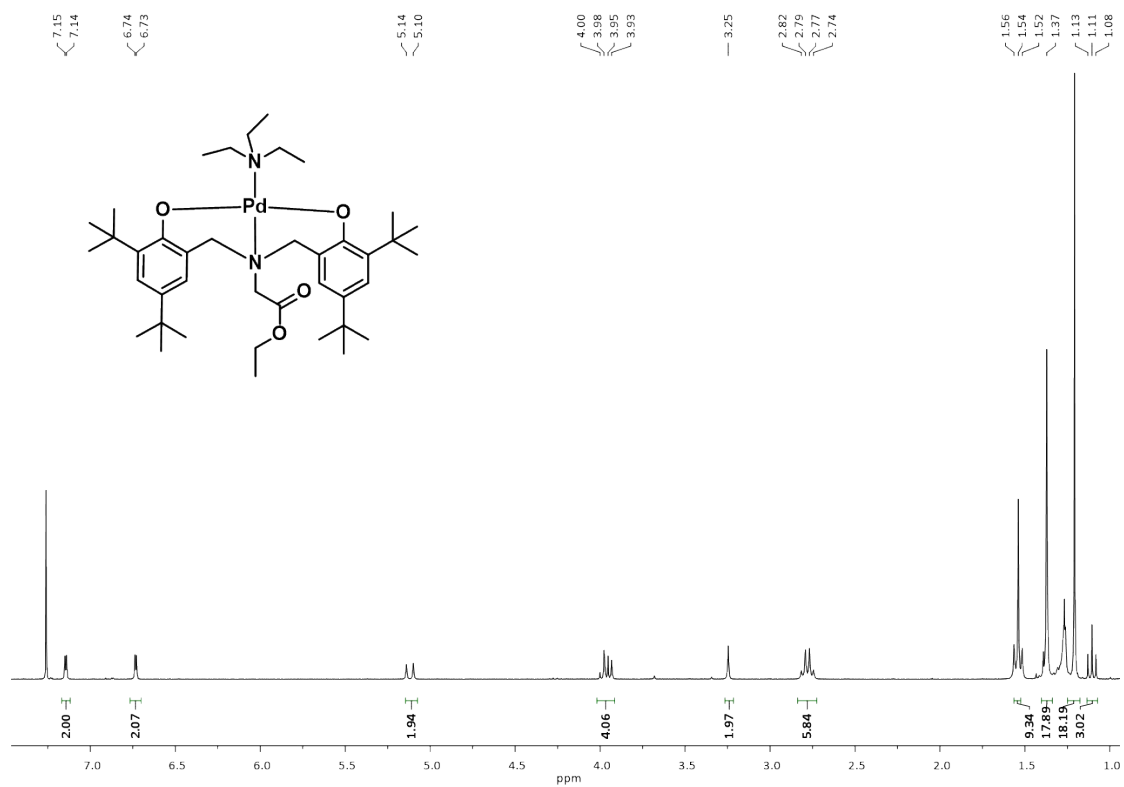


Figure S24. ^1H NMR spectrum of C1 (300 MHz, CDCl_3 at 298 K).

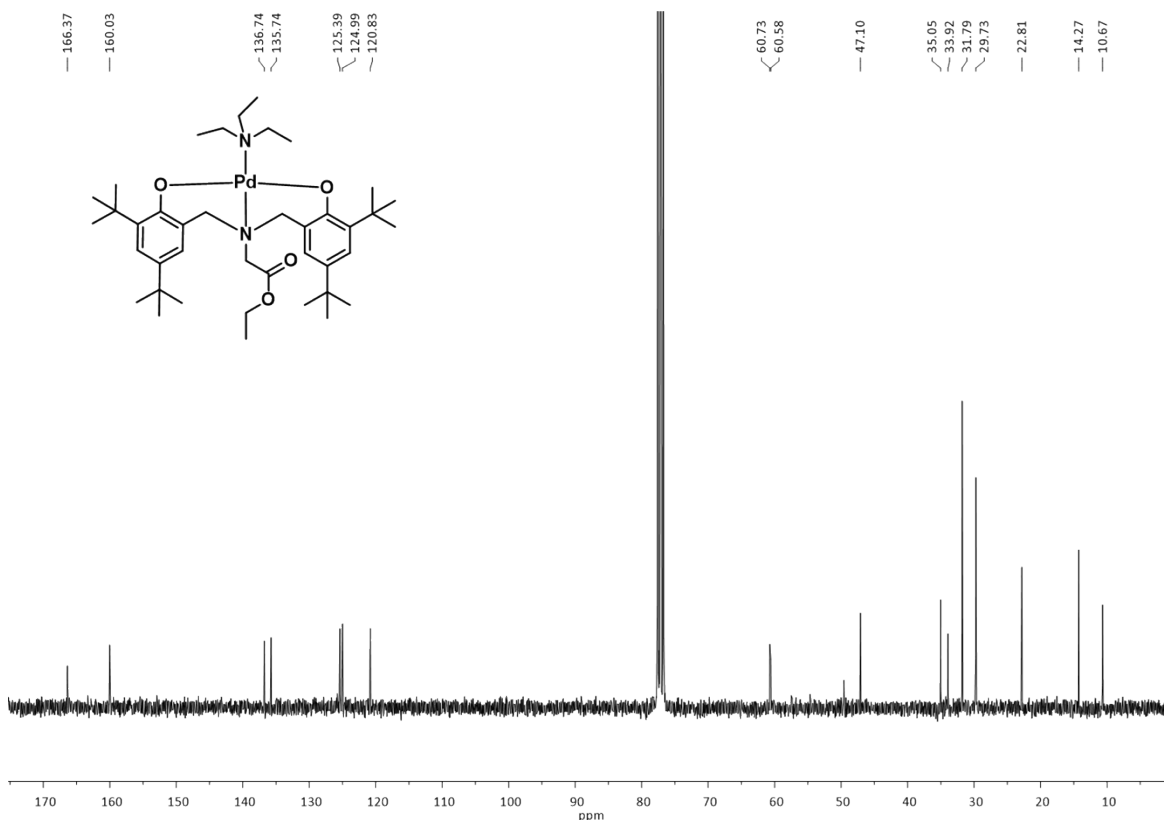


Figure S25. ^{13}C NMR spectrum of C1 (75 MHz, CDCl_3 at 298 K).

C2



Figure S26. ¹H NMR spectrum of **C2** (300 MHz, CDCl₃ at 298 K).

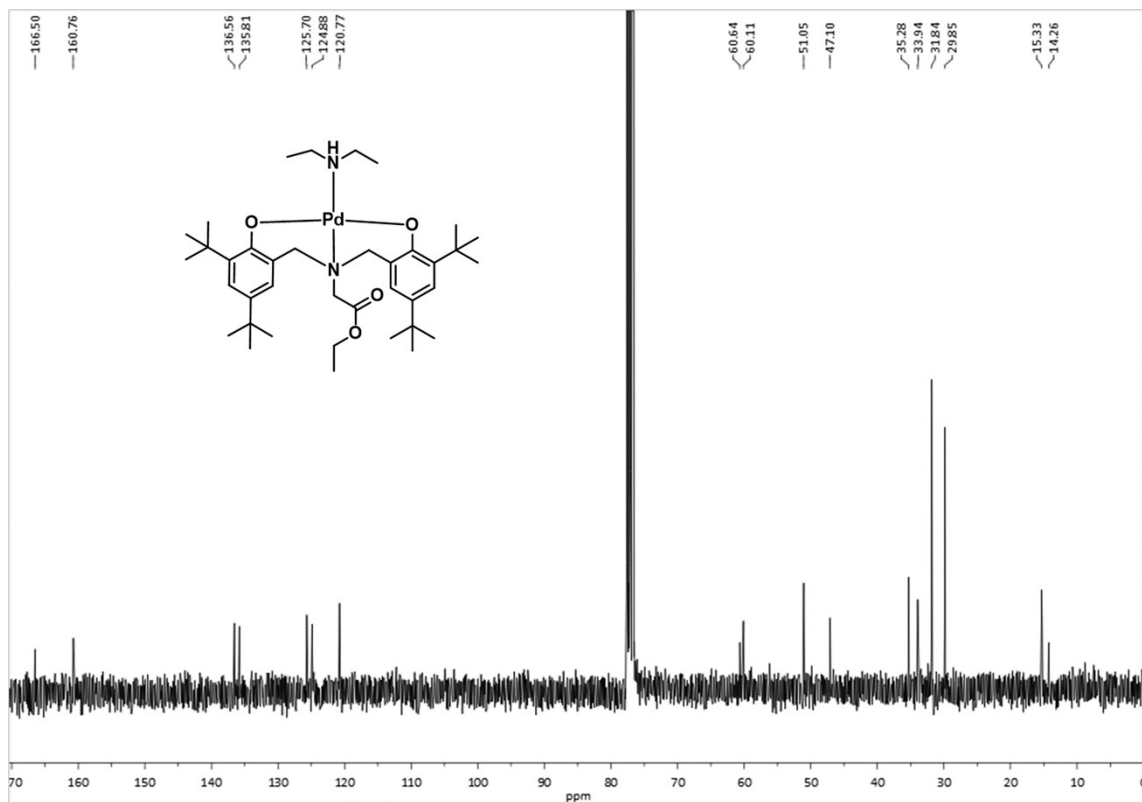


Figure S27. ¹³C NMR spectrum of **C2** (75 MHz, CDCl₃ at 298 K).

C3

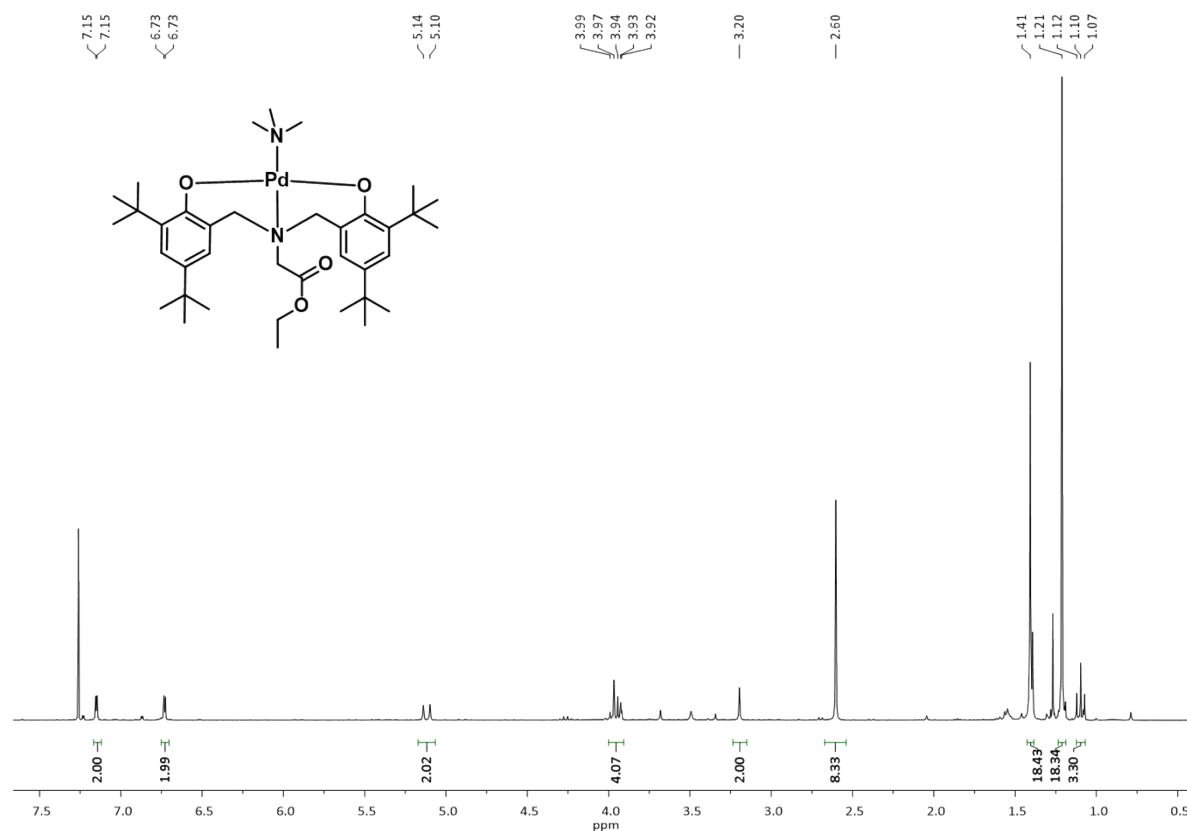


Figure S28. ¹H NMR spectrum of C3 (300 MHz, CDCl₃ at 298 K).

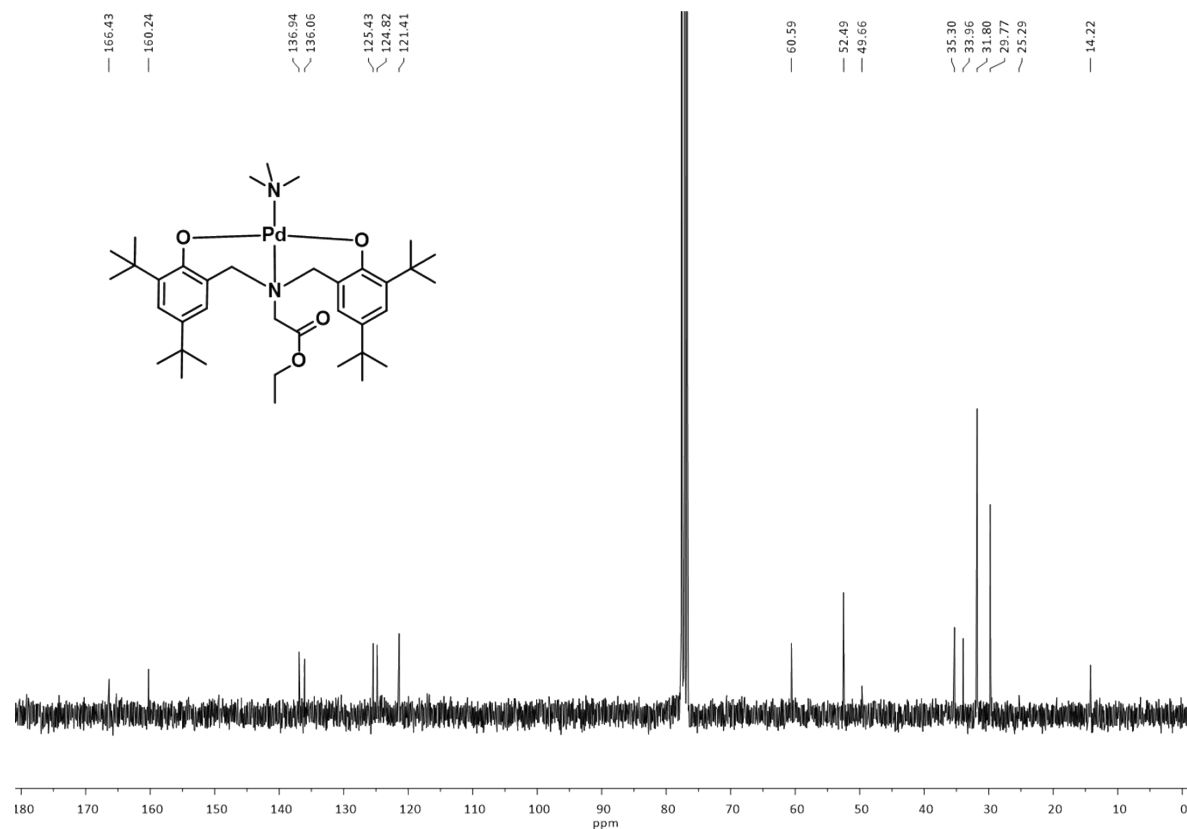


Figure S29. ¹³C NMR spectrum of C3 (75 MHz, CDCl₃ at 298 K).

C4



Figure S30. ¹H NMR spectrum of C4 (300 MHz, CDCl₃ at 298 K).

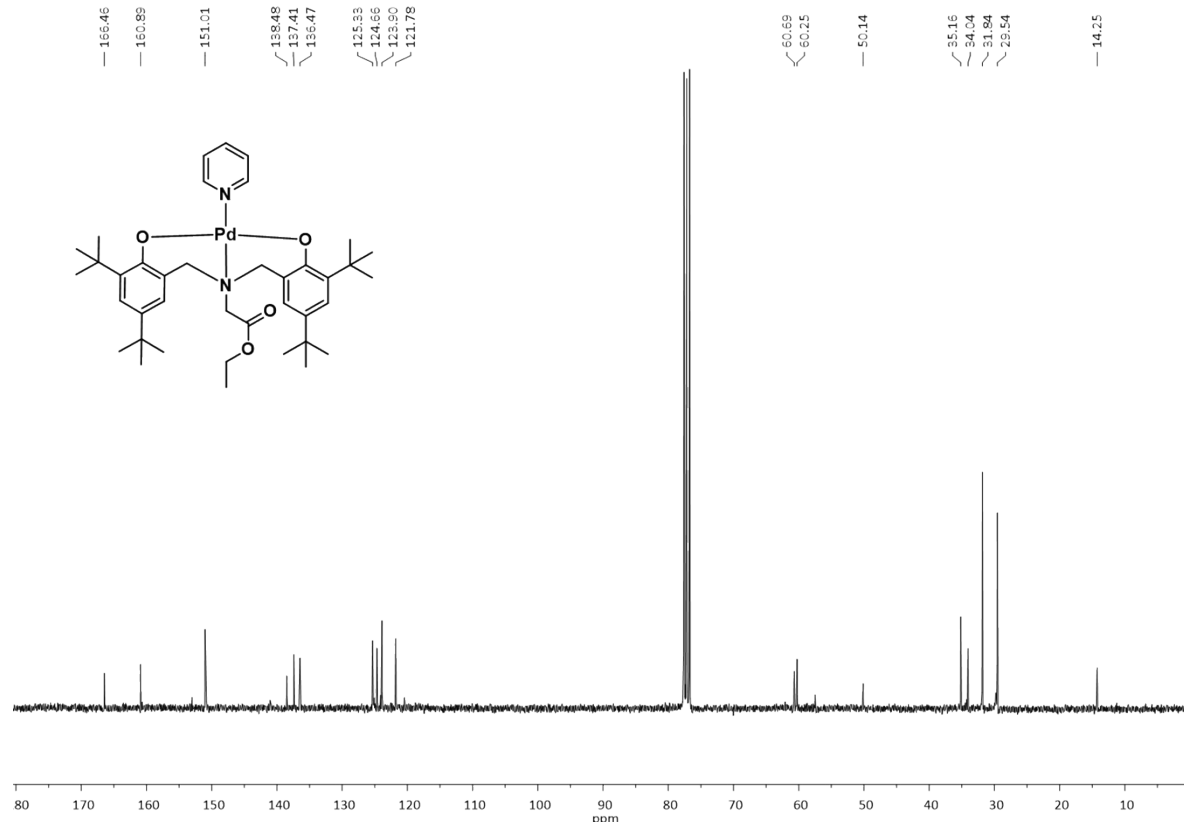


Figure S31. ¹³C NMR spectrum of C4 (75 MHz, CDCl₃ at 298 K).

C5

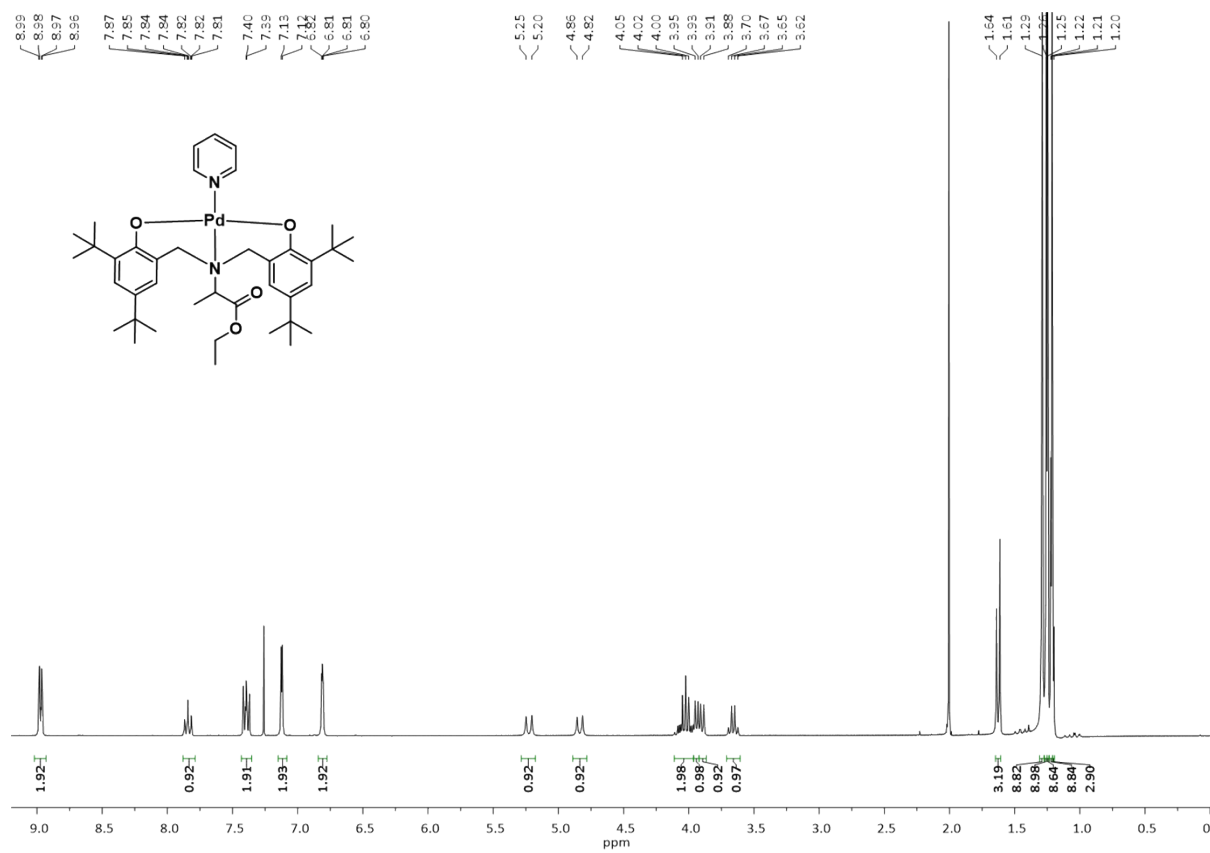


Figure S32. ¹H NMR spectrum of C5 (300 MHz, CDCl₃ at 298 K).

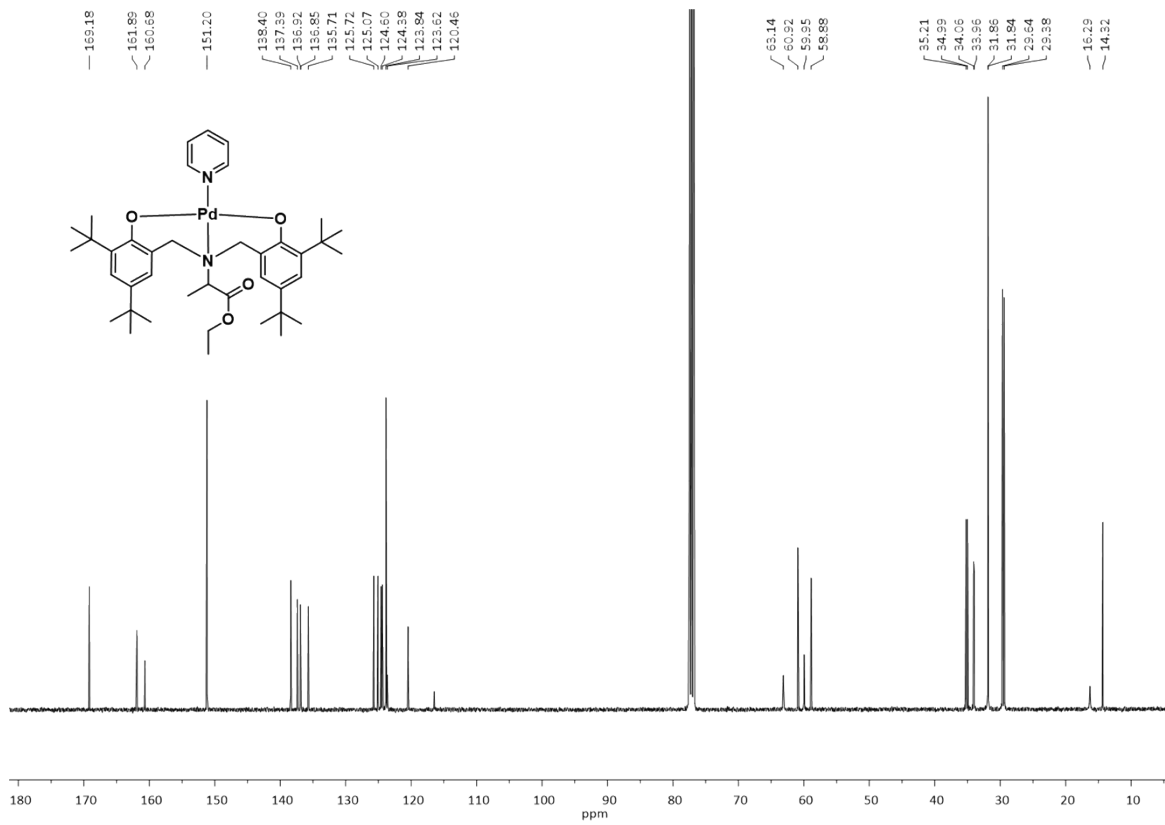


Figure S33. ¹³C NMR spectrum of C5 (75 MHz, CDCl₃ at 298 K).

C6

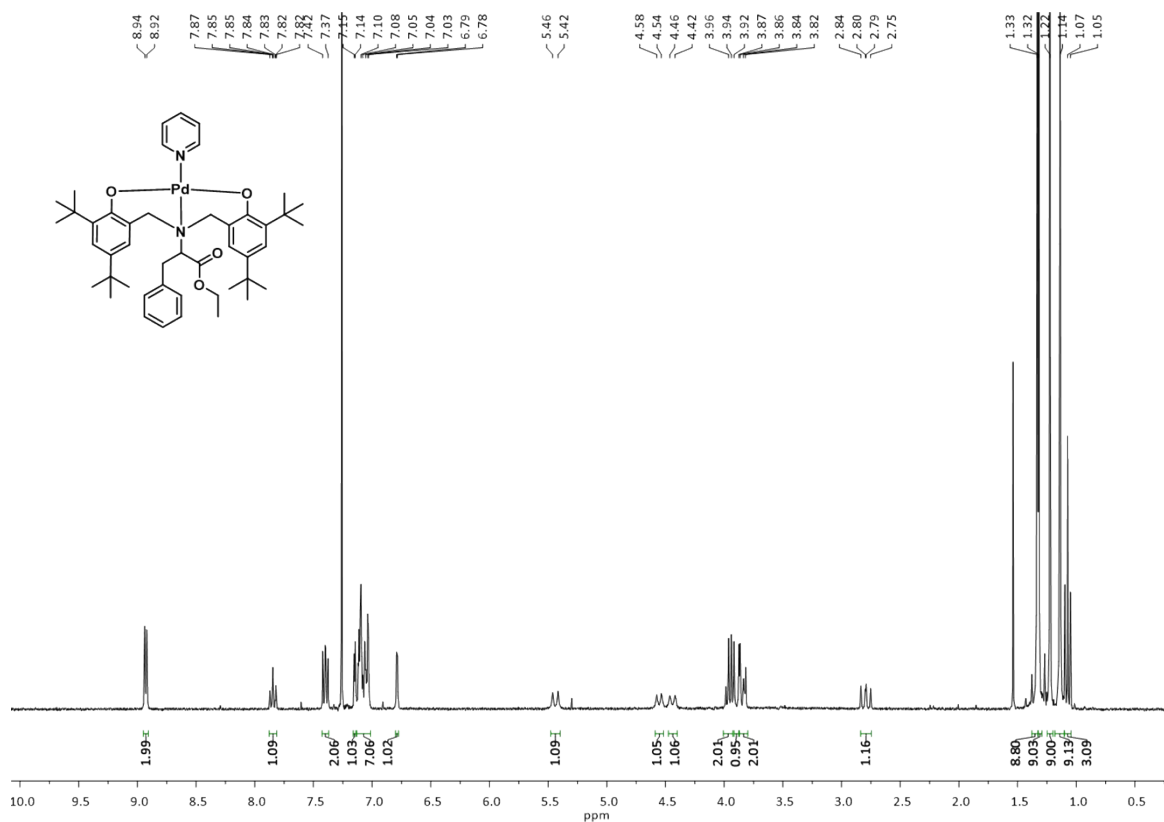


Figure S34. ¹H NMR spectrum of **C6** in CDCl₃ (300 MHz, CDCl₃ at 298 K).

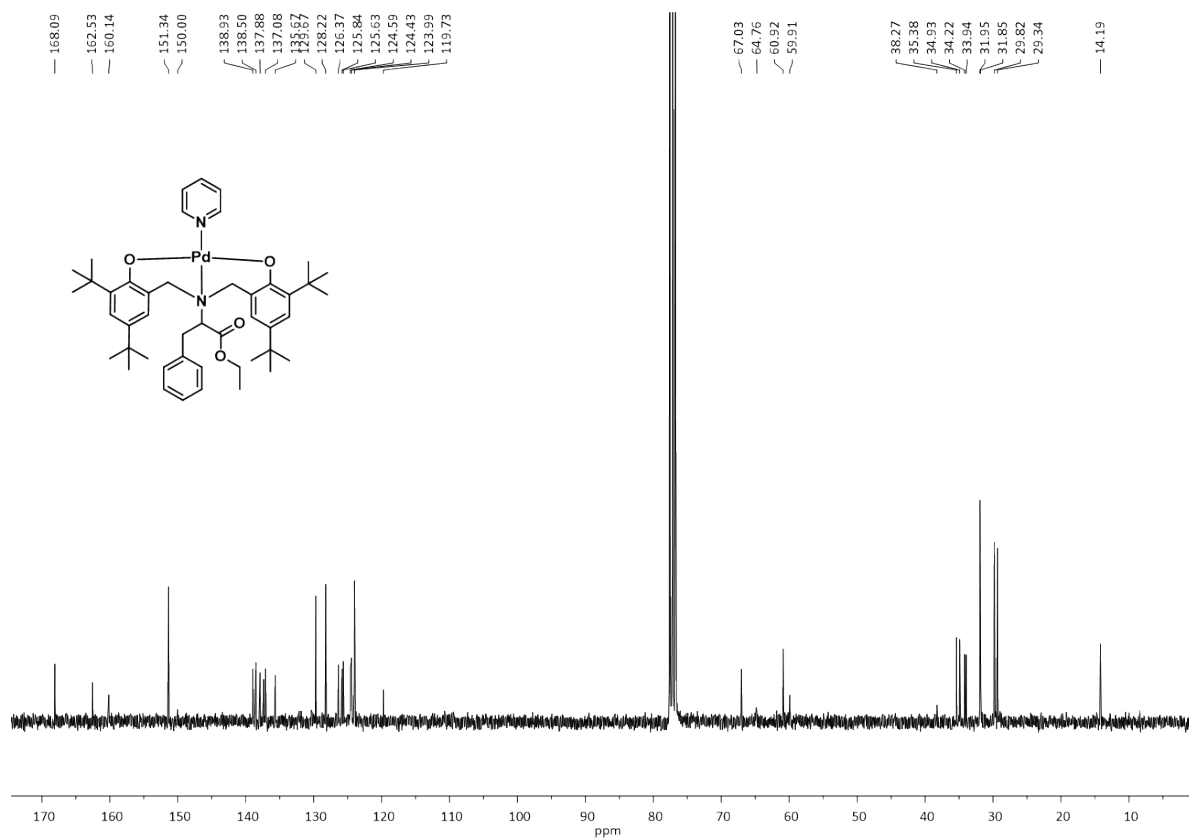


Figure S35. ¹³C NMR spectrum of **C6** (75 MHz, CDCl₃ at 298 K).

C7

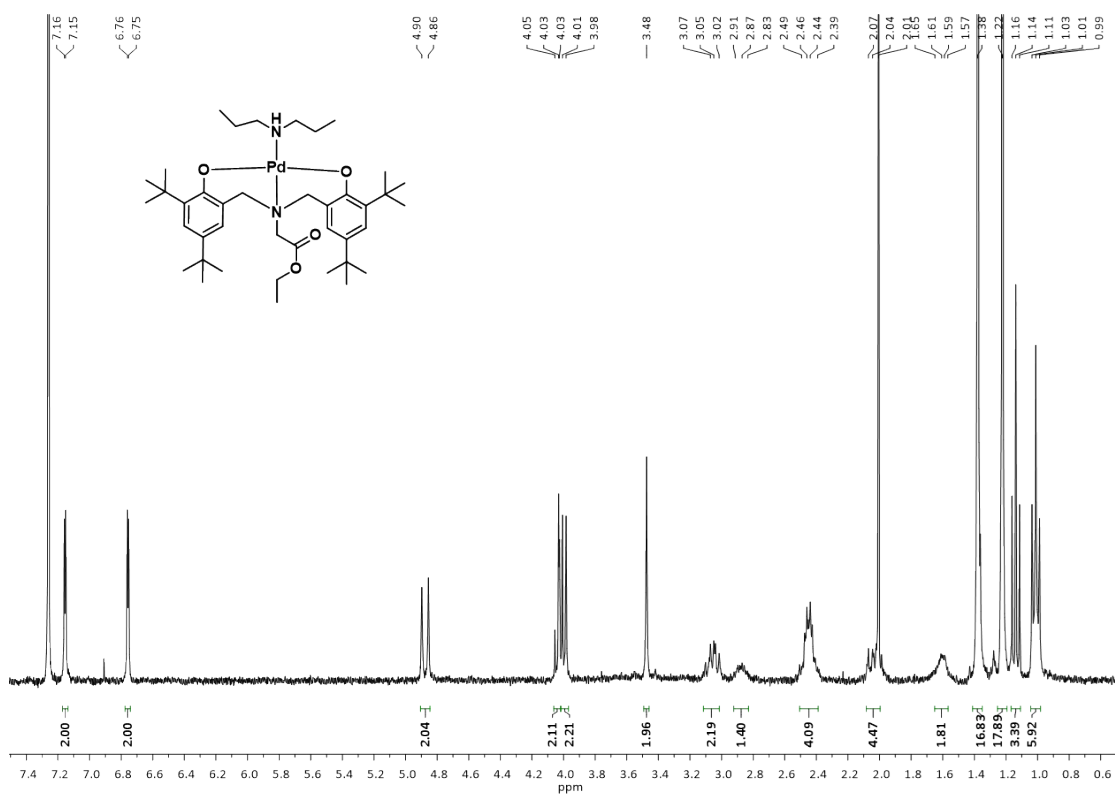


Figure S36. ¹H NMR spectrum of C7 (300 MHz, CDCl₃ at 298 K).

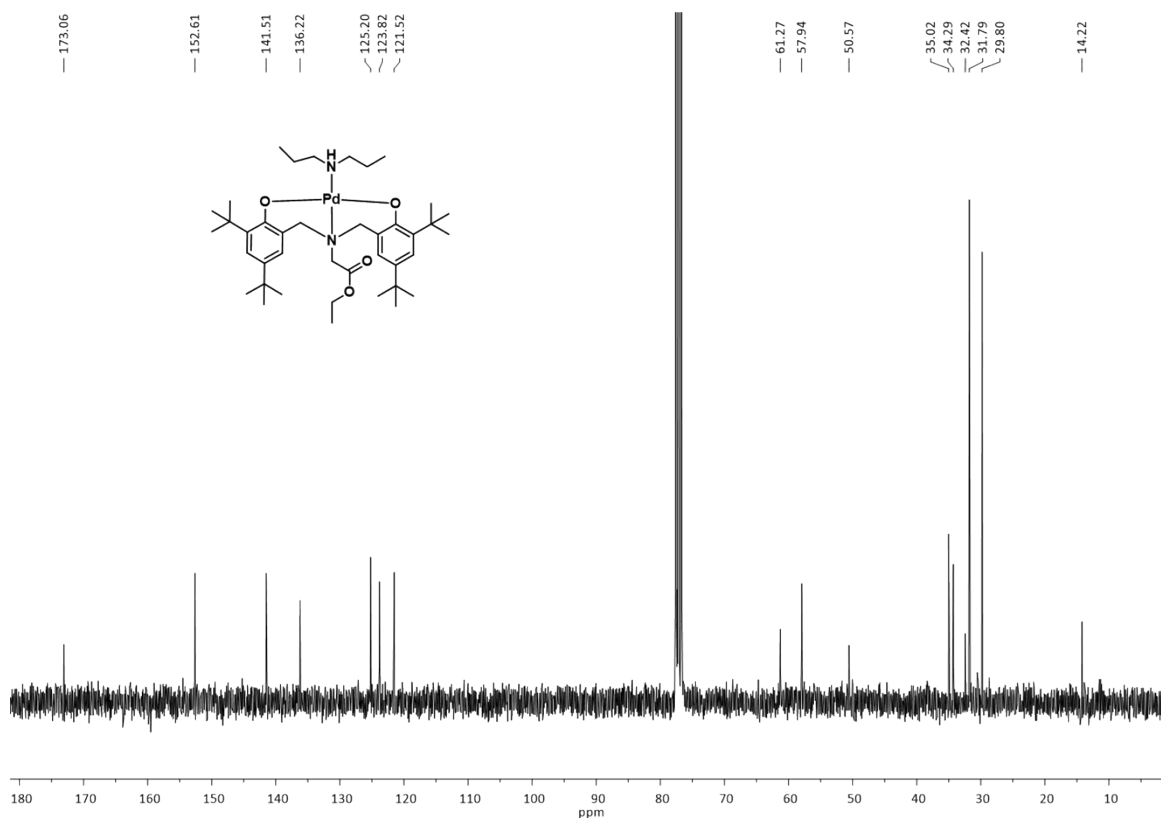


Figure S37. ¹³C NMR spectrum of C7 (75 MHz, CDCl₃ at 298 K).

6. ESI High Resolution Mass Spectrometry data of Pd complexes C1-C7

C1

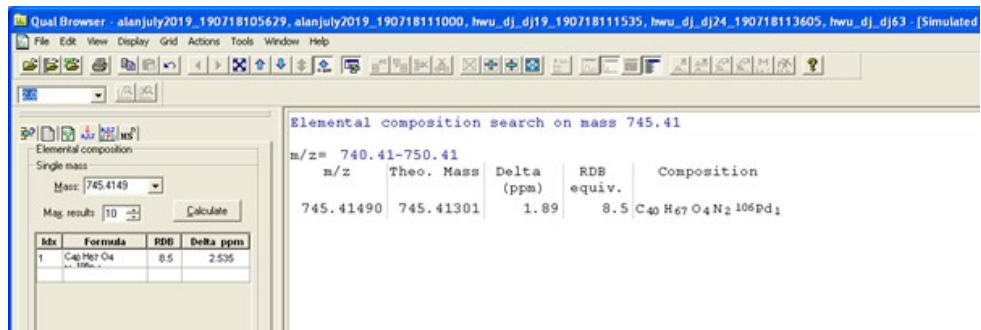


Figure S38. HRMS data of C1.

C2

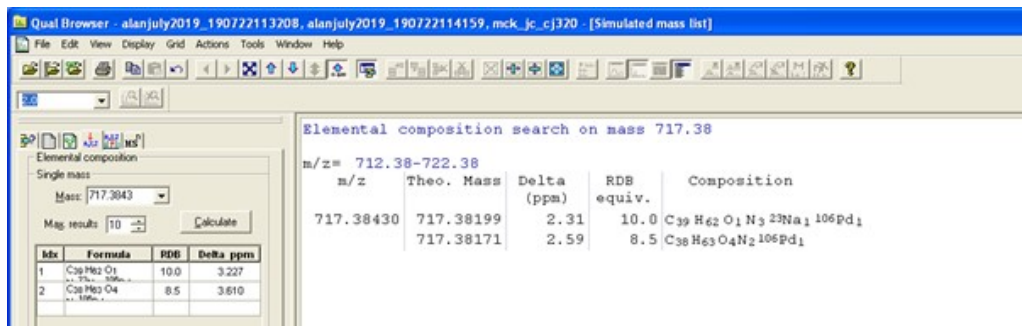


Figure S39. HRMS data of C2.

C3

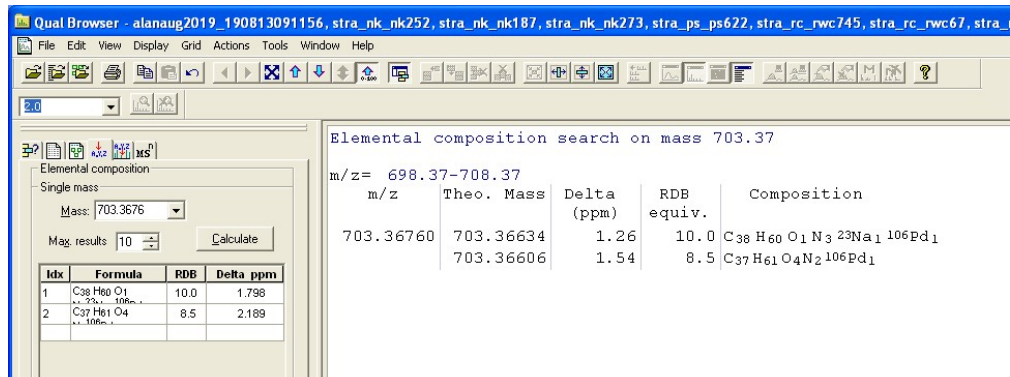


Figure S40. HRMS data of C3.

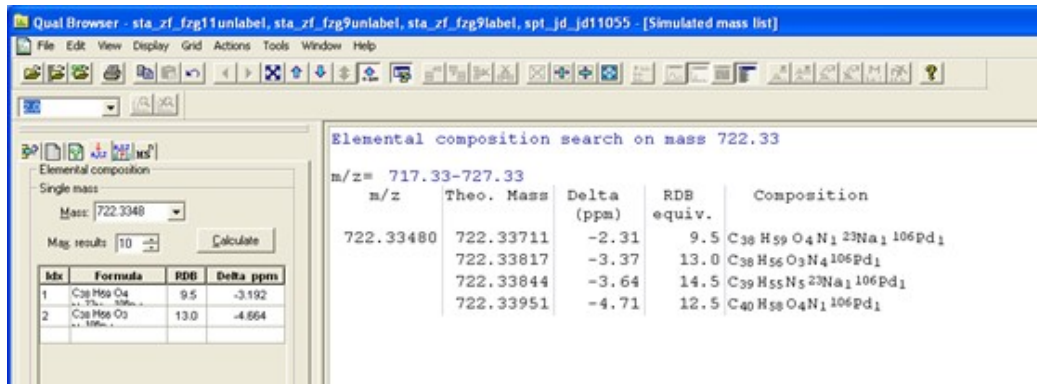
C4

Figure S41. HRMS data of C4.

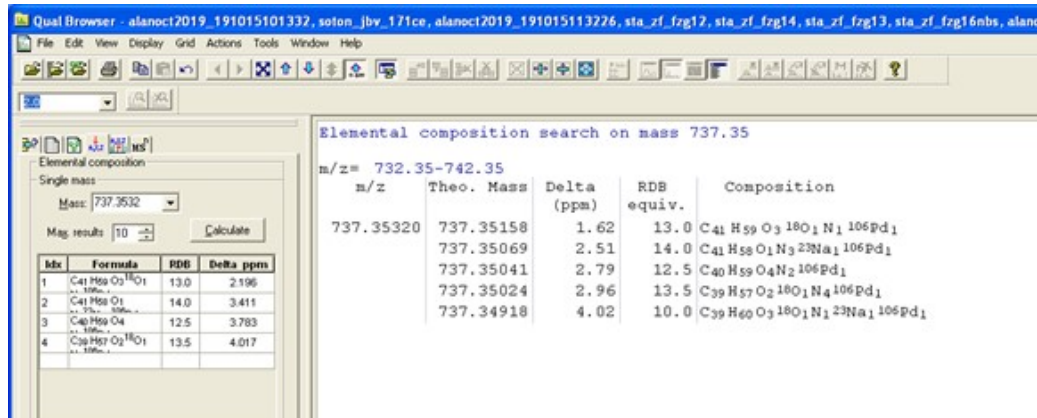
C5

Figure S42. HRMS data of C5.

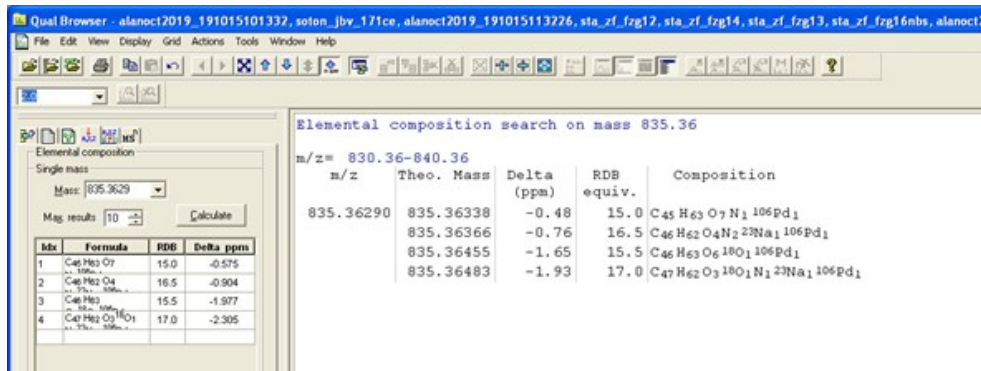
C6

Figure S43. HRMS data of C6.

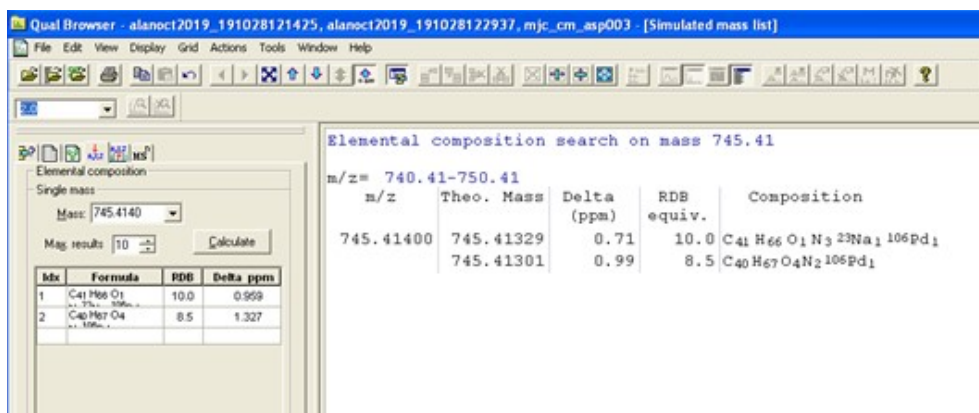
C7

Figure S44. HRMS data of C7.

7. Typical ^1H NMR spectra of Suzuki-Miyaura and Mizoroki-Heck crude reaction mixtures

Suzuki-Miyaura reactions:

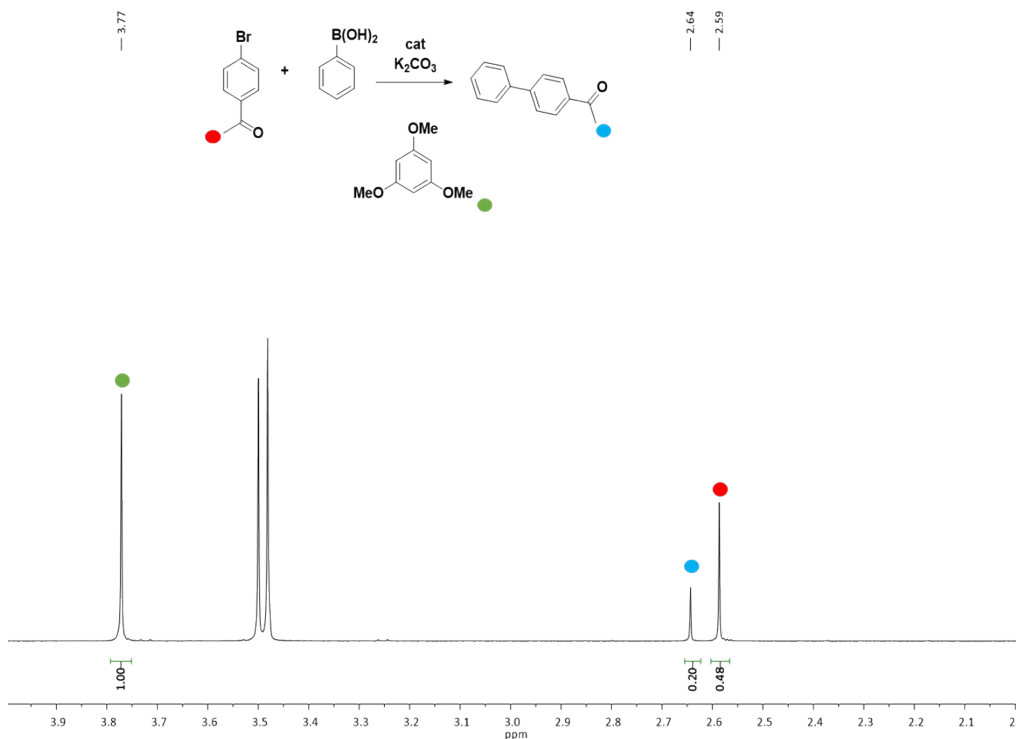
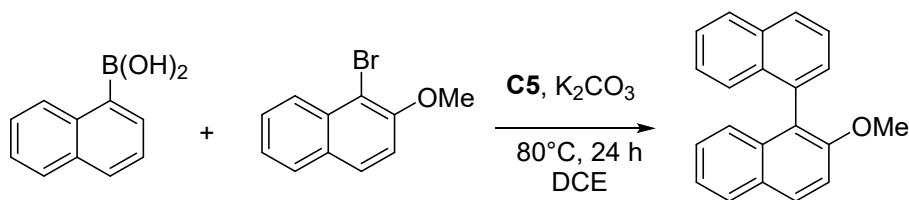


Figure S45. Typical ^1H NMR spectrum (298 K, CDCl_3 , 300 MHz) of a Suzuki-Miyaura reaction mixture indicating the CH_3 shifts of starting material (4'-bromoacetophenone, 2.59 ppm, red), product (4-acetyl biphenyl, 2.64 ppm, blue) and internal standard (1,3,5-trimethoxybenzene, 3.77 ppm, green).¹

Substrate scope:

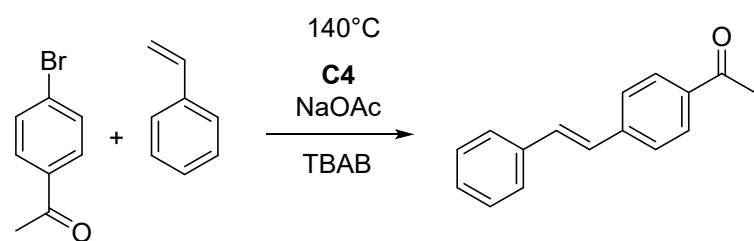
All aryl-halides tested in the Suzuki-Miyaura coupling reactions with phenylboronic acid using catalyst **C4** afforded known biaryl species with reported full characterisations. Conversions were calculated via ^1H NMR, integrating the internal standard peak (1,3,5-trimethoxybenzene, 3.77 ppm) against product peaks matched with literature values for bromo-4-nitrobenzene,² 4-bromoaniline,³ 4-bromo-2-fluoronitrobenzene,⁴ 1-bromo-2-methoxynaphthalene,⁵ 1-bromo-4-^tBu-benzene,⁶ 1-bromotoluene, 2-bromotoluene and 3-bromotoluene.⁷

Asymmetric reaction:



Scheme S1. Suzuki-Miyaura coupling of 1-naphthaleneboronic acid and 1-bromo-2-methoxynaphthalene.

Mizoroki-Heck reactions:



Scheme S2. Mizoroki-Heck reaction of 4'-bromoacetophenone and styrene.

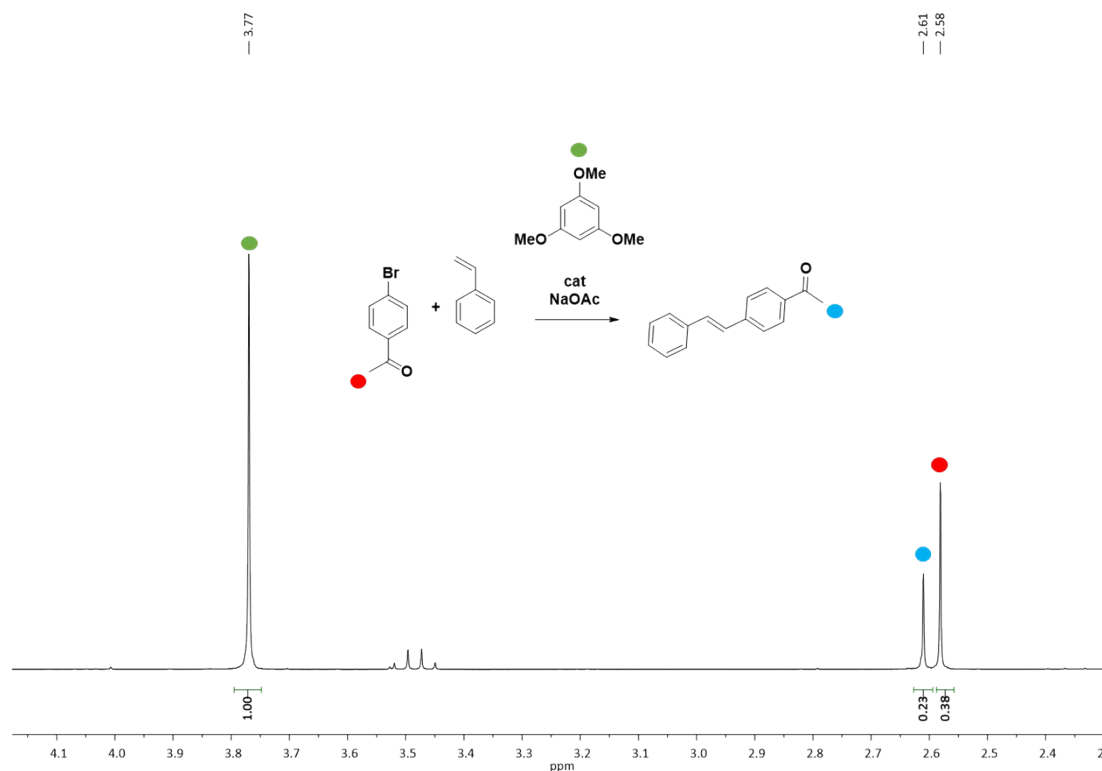


Figure S46. Typical ¹H NMR spectrum (298 K, CDCl₃, 300 MHz) of a Heck-Mizoroki reaction mixture indicating the CH₃ shifts of starting material (4'-bromoacetophenone, 2.59 ppm, red), product (4-acetylstilbene, 2.61 ppm, blue) and internal standard (1,3,5-trimethoxybenzene, 3.77 ppm, green).⁸

8. Crystallographic data and refinement details for ligands L1-L6 (Table S1) and Complexes C1-C6 (Table S2)

Table S1. Crystallographic data and refinement details for ligands **L1-L6**.

Identification code	L1	L2	L3	L4	L5	L6
CCDC number	2070846	2070847	2070849	2070850	2070851	2070853
Empirical formula	C _{34.5} H ₅₄ NO ₄ Cl	C ₃₅ H ₅₅ NO ₄	C ₄₁ H ₅₉ NO ₄	C ₂₃ H ₃₁ Cl ₂ NO ₄	C ₂₃ H ₃₁ NO ₄	C ₃₀ H ₃₇ Cl ₂ NO ₄
Formula weight	582.23	553.8	629.89	456.39	385.49	546.5
Temperature/K	100	100	100	100	100	100
Crystal system	monoclinic	orthorhombic	orthorhombic	monoclinic	triclinic	monoclinic
Space group	P2 ₁ /c	P2 ₁ 2 ₁ 2 ₁	P2 ₁ 2 ₁ 2 ₁	C2/c	P-1	P2 ₁ /c
a/Å	14.4965(2)	9.08240(10)	10.4115(2)	22.1011(3)	10.5479(2)	14.3845(4)
b/Å	19.9546(3)	11.7694(2)	11.7529(2)	12.1705(2)	14.5535(3)	16.8171(4)
c/Å	12.0794(2)	31.5208(5)	31.8349(5)	17.0857(3)	15.4442(3)	11.7263(3)
α/°	90	90	90	90	70.3610(10)	90
β/°	103.8657(8)	90	90	92.1340(10)	70.5070(10)	99.9650(10)
γ/°	90	90	90	90	76.5600(10)	90
Volume/Å ³	3392.41(9)	3369.40(9)	3895.49(12)	4592.55(13)	2085.52(7)	2793.86(13)
Z	4	4	4	8	4	4
ρ _{calcg/cm³}	1.14	1.092	1.074	1.32	1.228	1.299
μ/mm ⁻¹	1.269	0.543	0.525	0.312	0.667	2.375
F(000)	1268	1216	1376	1936	832	1160
Crystal size/mm ³	0.28 × 0.22 × 0.06	0.4 × 0.36 × 0.12	0.25 × 0.18 × 0.14	0.3 × 0.2 × 0.2	0.32 × 0.2 × 0.16	0.32 × 0.04 × 0.04
Radiation	CuKα (λ = 1.54178)	CuKα (λ = 1.54178)	CuKα (λ = 1.54178)	MoKα (λ = 0.71073)	CuKα (λ = 1.54184)	CuKα (λ = 1.54178)
2θ range for data coll./°	6.28 to 140.358	5.608 to 144.242	8.018 to 136.742	5.922 to 54.202	6.328 to 145.126	6.238 to 153.202
Index ranges	-17 ≤ h ≤ 16, -24 ≤ k ≤ 24, -14 ≤ l ≤ 14	-11 ≤ h ≤ 11, -14 ≤ k ≤ 14, -38 ≤ l ≤ 38	-12 ≤ h ≤ 12, -14 ≤ k ≤ 14, -36 ≤ l ≤ 38	-27 ≤ h ≤ 28, -15 ≤ k ≤ 15, - 21 ≤ l ≤ 21	-13 ≤ h ≤ 13, -17 ≤ k ≤ 16, - 19 ≤ l ≤ 18	-17 ≤ h ≤ 17, -20 ≤ k ≤ 20, - 14 ≤ l ≤ 14
Reflections collected	46320	47117	48693	42089	24899	33650
Independent reflections	6446 [R _{int} = 0.0405, R _{sigma} = 0.0216]	6637 [R _{int} = 0.0279, R _{sigma} = 0.0151]	7128 [R _{int} = 0.0419, R _{sigma} = 0.0219]	5056 [R _{int} = 0.0306, R _{sigma} = 0.0158]	8049 [R _{int} = 0.0550, R _{sigma} = 0.0542]	5696 [R _{int} = 0.0739, R _{sigma} = 0.0472]
Data/restraints/parameters	6446/0/448	6637/0/377	7128/1/441	5056/12/311	8049/0/521	5696/0/341
Goodness-of-fit on F ²	1.052	1.036	1.087	1.045	1.078	1.046
Final R indexes [I>=2σ (I)]	R ₁ = 0.0415, wR ₂ = 0.1016	R ₁ = 0.0262, wR ₂ = 0.0693	R ₁ = 0.0567, wR ₂ = 0.1615	R ₁ = 0.0417, wR ₂ = 0.1168	R ₁ = 0.0494, wR ₂ = 0.1295	R ₁ = 0.0631, wR ₂ = 0.1566
Final R indexes [all data]	R ₁ = 0.0477, wR ₂ = 0.1065	R ₁ = 0.0265, wR ₂ = 0.0696	R ₁ = 0.0583, wR ₂ = 0.1632	R ₁ = 0.0493, wR ₂ = 0.1237	R ₁ = 0.0716, wR ₂ = 0.1405	R ₁ = 0.0814, wR ₂ = 0.1719
Largest diff. peak/hole/e Å ⁻³	0.30/-0.25	0.27/-0.16	1.34/-0.21	0.38/-0.59	0.22/-0.25	0.37/-0.82

Table S2. Crystallographic data and refinement details for complexes **C1-C6**.

Identification code	C1	C2	C3	C4	C5	C6
CCDC number	2063653	2063654	2060147	2060195	2060200	2060206
Empirical formula	<chem>C40H66N2O4Pd</chem>	<chem>C41H69.5N2O4Pd</chem>	<chem>C36.66H59.32N2O4Pd</chem>	<chem>C39H56N2O4Pd</chem>	<chem>C42H61N3O4Pd</chem>	<chem>C46H62N2O4Pd</chem>
Formula weight	745.34	760.88	698.5	723.25	778.33	813.37
Temperature/K	100	100	100	100	100	100
Crystal system	monoclinic	monoclinic	triclinic	monoclinic	orthorhombic	monoclinic
Space group	Pn	C2/c	P-1	P2 ₁ /c	Pna2 ₁	P2 ₁
a/Å	9.9356(4)	27.3384(7)	10.8890(2)	23.5009(5)	18.1718(8)	13.3749(3)
b/Å	26.4605(11)	9.7533(2)	11.7145(3)	5.88070(10)	11.3807(4)	10.4918(2)
c/Å	15.5658(6)	31.2674(8)	15.3877(3)	28.0066(6)	20.0056(7)	16.3394(3)
$\alpha/^\circ$	90	90	103.1830(10)	90	90	90
$\beta/^\circ$	105.0420(10)	96.1430(10)	104.3440(10)	106.1280(10)	90	112.5780(10)
$\gamma/^\circ$	90	90	99.5060(10)	90	90	90
Volume/Å ³	3952.0(3)	8289.3(3)	1799.70(7)	3718.23(13)	4137.3(3)	2117.13(7)
Z	4	8	2	4	4	2
$\rho_{\text{calc}}/\text{cm}^3$	1.253	1.219	1.289	1.292	1.25	1.276
μ/mm^{-1}	0.509	3.908	4.456	4.336	3.94	3.867
F(000)	1592	3260	743	1528	1648	860
Crystal size/mm ³	0.3 × 0.2 × 0.2	0.22 × 0.08 × 0.04	0.18 × 0.06 × 0.04	0.38 × 0.04 × 0.04	0.38 × 0.10 × 0.06	0.1 × 0.03 × 0.03
Radiation	MoKα ($\lambda = 0.71073$)	CuKα ($\lambda = 1.54178$)	CuKα ($\lambda = 1.54178$)	CuKα ($\lambda = 1.54178$)	CuKα ($\lambda = 1.54178$)	CuKα ($\lambda = 1.54178$)
2θ range for data coll./°	5.354 to 52.802	5.686 to 119.832	6.178 to 149.518	6.57 to 149.684	10.18 to 150.324	10.86 to 149.778
Index ranges	-12 ≤ h ≤ 12, -33 ≤ k ≤ 33, -19 ≤ l ≤ 19	-29 ≤ h ≤ 30, -10 ≤ k ≤ 10, -33 ≤ l ≤ 34	-13 ≤ h ≤ 13, -13 ≤ k ≤ 14, -19 ≤ l ≤ 19	-29 ≤ h ≤ 29, -7 ≤ k ≤ 7, -34 ≤ l ≤ 35	-22 ≤ h ≤ 22, -14 ≤ k ≤ 14, -25 ≤ l ≤ 25	-16 ≤ h ≤ 15, -13 ≤ k ≤ 13, -20 ≤ l ≤ 20
Reflections collected	146440	44289	141515	81773	55090	56149
Independent reflections	15877 [R _{int} = 0.0551, R _{sigma} = 0.0239]	6054 [R _{int} = 0.0382, R _{sigma} = 0.0249]	7359 [R _{int} = 0.0707, R _{sigma} = 0.0224]	7626 [R _{int} = 0.0323, R _{sigma} = 0.0167]	8373 [R _{int} = 0.0409, R _{sigma} = 0.0277]	8347 [R _{int} = 0.0358, R _{sigma} = 0.0312]
Data/restraints/parameters	15877/7/905	6054/1/462	7359/0/414	7626/0/428	8373/7/498	8347/1/492
Goodness-of-fit on F ²	1.057	1.039	1.058	1.05	1.054	1.035
Final R indexes [$ I >=2\sigma(I)$]	R ₁ = 0.0293, wR ₂ = 0.0646	R ₁ = 0.0271, wR ₂ = 0.0639	R ₁ = 0.0429, wR ₂ = 0.0870	R ₁ = 0.0217, wR ₂ = 0.0567	R ₁ = 0.0199, wR ₂ = 0.0515	R ₁ = 0.0179, wR ₂ = 0.0444
Final R indexes [all data]	R ₁ = 0.0314, wR ₂ = 0.0656	R ₁ = 0.0316, wR ₂ = 0.0664	R ₁ = 0.0483, wR ₂ = 0.0900	R ₁ = 0.0229, wR ₂ = 0.0576	R ₁ = 0.0201, wR ₂ = 0.0516	R ₁ = 0.0180, wR ₂ = 0.0444
Largest diff. peak/hole/e Å ⁻³	0.56/-0.47	0.43/-0.56	1.25/-1.37	0.39/-0.72	0.37/-0.99	0.35/-0.49

10. References

1. A. K. Bowser, A. M. Anderson-Wile, D. H. Johnston and B. M. Wile, *Appl. Organomet. Chem.*, 2016, **30**, 32-39.
2. S.-D. Cho, H.-K. Kim, H.-s. Yim, M.-R. Kim, J.-K. Lee, J.-J. Kim and Y.-J. Yoon, *Tetrahedron*, 2007, **63**, 1345-1352.
3. E. Alacid and C. Nájera, *Org. Lett.*, 2008, **10**, 5011-5014.
4. D.-D. Li, W.-L. Chen, X.-L. Xu, F. Jiang, L. Wang, Y.-Y. Xie, X.-J. Zhang, X.-K. Guo, Q.-D. You and H.-P. Sun, *Eur. J. Med. Chem.*, 2016, **118**, 1-8.
5. H. Li, Y. Wu and W. Yan, *J. Organomet. Chem.*, 2006, **691**, 5688-5696.
6. H. Li, C.-L. Sun, M. Yu, D.-G. Yu, B.-J. Li and Z.-J. Shi, *Chem. Eur. J.*, 2011, **17**, 3593-3597.
7. D. Zhang, L. Le, R. Qiu, W.-Y. Wong and N. Kambe, *Angew. Chem. Int. Ed.*, 2021, **60**, 3104-3114.
8. L.-C. Liu, Y.-H. Tzeng, C.-H. Hung and H. M. Lee, *Eur. J. Inorg. Chem.*, 2020, 3601-3611.